NRIAG JOURNAL OF ASTRONOMY AND GEOPHYSICS
2020, VOL. 9, NO. 1, 129–154
https://doi.org/10.1080/20909977.2020.1727674

3-D static modelling of lateral heterogeneity using geostatistics and artificial neural network in reservoir characterisation of "P" field, Niger Delta

Akindeji Opeyemi Fajana

Department of Geophysics, Federal University Oye, Oye, Nigeria

ABSTRACT

The anisotropic and heterogeneous nature of the subsurface units at offset wells gets more complex at locations outside well control. However, qualitative and quantitative predictions of reservoir properties and geometries beyond well control are vital to understanding the intrinsic characteristics of subsurface formations. Supervised Multi-layer Perceptron neural network and conditional sequential Gaussian simulation were applied to a suite of well logs data set and three dimensional (3-D) seismic dataset acquired from P-field, Niger Delta to predict lateral continuity of hydrocarbon reservoir properties. Multilayer perceptron neural network was used to model effective porosity (Eϕ) at the root-mean-square error of 0.00531 with an estimated average effective porosity of 0.2952. Furthermore, MLPNN modelling of hydrocarbon saturation (S_h) at root mean square error of 0.02821 yielded an estimated average of 69.73%. The volume of shale (V_{sh}) was also modelled at the root mean square error of 0.0282, with an estimated Vsh average of 9% for the study area. It was discovered that a comparatively higher net-to-gross (N-T-G), relatively higher effective porosity, high hydrocarbon saturation, very low volume of shale, and high permeability were observed in the areas of interest in the study area. A geostatistical approach was also used to model petrophysical properties. The parametric semivariogram model shows the range of 94–5230 m, nugget effect of 0.062, and sills of 0.075, 0.093, and 0.0121. Realisations were generated and ranked using the SGS algorithm suggest that any one of the realisations can independently represent the real picture of the subsurface geology within the study area. The integration of these different prediction tools and analyses of the outcomes from the research has improved our understanding of delineated reservoirs and improved lateral variation prediction of its properties. These prediction tools served better as a complementary tool to each other rather than as a comparison tool.

ARTICLE HISTORY
Received 7 February 2019
Revised 26 January 2020
Accepted 31 January 2020

KEYWORDS
Hydrocarbon; inversion; uncertainties; porosity; reserves

1. Preamble

Reservoirs are sampled directly or indirectly by the use of various geophysical exploration techniques, which gives a presentation that is a function of the data from which characterisation can be carried out. A major challenge in hydrocarbon exploration lies in need for proper mapping of the reservoir and its characterisation to determine the economic value of such a field. Characterisation in a hydrocarbon reservoir and its petrophysical properties in detail, such that the properties upon which the descriptions are made have coefficients unique to the reservoir analysed. These properties are parameters that are either quantitatively or qualitatively derived from making good the total outlook of the reservoir while giving a clear and reliable indication of its hydrocarbon potential. Moreover, in reserve estimation and planning production operations, hydrocarbon reservoir characterisation is essential and has played an important role in reservoir studies, the evaluation of which could be for different purposes. Its success can greatly enhance a variety of decisions to be made in various fields in which it is applicable, most importantly in hydrocarbon exploration. The goal of any reservoir characterisation is to typify the nature of the reservoir and to have first-hand and reliable information peculiar to it. Most of the time, due to the inaccessibility of the reservoir of interest, predictive variables are adopted in projects. Reservoirs are sampled directly or indirectly by the use of various geophysical exploration techniques, which give a presentation that is a function of the data from which characterisation can be carried out. Nonetheless, properties of hydrocarbon-bearing reservoirs such as water saturation, net-to-gross, porosity, and hydrocarbon saturation can be estimated from borehole log data interpretation. Integration of log calculated reservoir properties and seismic amplitude analysis and seismic structural interpretation can aid an interpreter to quantify subsurface petroleum resources and accumulations, classify petroleum resources, delineate prospects and leads, calculate probability of success, rank available petroleum resources, design appraisal, and developmental wells, minimise risks in exploration and exploitation, and also boost success rate for exploitable prospects. Due to these reasons, this study exemplifies

CONTACT Akindeji Opeyemi Fajana, akindeji.fajana@fuoye.edu.ng, Department of Geophysics, Federal University Oye, Oye, Ekiti State, Nigeria

how geophysical methods can help to maximise recovery by identifying bypass reservoir zones and heterogeneities that control hydrocarbon recovery. Since rocks have elastic properties, the response of different rock materials to elastic waves based on density and the velocity of motion constitutes the root of the theories. Seismic records come with attributes that are intrinsic to the investigated terrains. Thus, there is a desire to know the information contained in the wavelet and also how to extract and use the same to characterise the rock unit (reservoir) (Caers, 2003). The lack of data and the delicate nature of the few at hand coupled with the significant need to come out with a valid and unassuming exploration philosophy for a particular terrain has informed the need to adequately look inward and properly take into consideration all the properties of the data set available and judiciously incorporate one into another. Models that are standard and peculiar to cases often result from an interpretation carefully done from a robust database that has taken into consideration the provenance and current properties of the analysed rock body. This study applies multi-attribute transforms and geostatistical inversion to the three-dimension (3D) seismic dataset and set of borehole logs data to predict lateral homogeneity of reservoir properties as well as quantifying the uncertainty associated with the predictions in the study area. Moreover, according to Chambers and Yarus (2002), the trend is towards the interpretation of single or combined data for lateral prediction of lithology, facies, petrophysical parameters, and other elastic properties of rocks such as coefficient of compressibility (shear modulus, μ), incompressible (bulk modulus, k), Poisson ratio (σ), Lames's constant (λ). Therefore, the geometric modelling of movement in hydrocarbon reservoirs necessitates the description of the physical properties and geometry of intricate geological formations. These can be modelled from few or low-resolution samples obtained from the borehole and seismic data and are required to be dependable with geological perceptions. A different approach for the integration of 3-D seismic data and borehole records is to use a multilayer perceptron neural network. The awareness of using many seismic attributes to predict borehole log properties was foremost projected by Schultz et al. (1994); Robinson (2001). Numerous case histories have been cited in the previous works for such prediction of borehole logs properties using multilinear stepwise regression and artificial neural networks (Russell et al. 1997; Skolen et al. 2006; Fogg 2000; Tonn 2002; Walls 2002; Pramanik et al. 2004). In this method, the training points are considered to be well to seismic ties. The relationship between attributes and borehole log data is derived, quantify, and quality check statistically. The method of cross justification is used to prevent "overtraining." It is essential to note that in these methods of multiattribute transforms, a precise solution is not enforced at well- to- seismic ties (Daniel et al. 2001), but a relationship of best fit is gotten at the tie points. This relationship is then used for the multiple inputs attributes to produce the reservoir property volume. Hampson et al. (2001), Strivastava (1994), and David et al. (2004) proposed combining both geostatistical and multiattribute transforms (linear or non-linear). The key to integrating seismic and well data is in establishing a significant correlation between them. If there is no correlation between seismic and well data, incorporation of the former will provide no additional information over what would be calculated with only the latter. When some correlations exist between seismic and well data, there will be some increase in the accuracy of the resulting map. The most important role of geostatistics in reservoir characterisation and modelling lies in the integration of data, providing a formalism to encode vital, possibly non-numerical facts; bring together different data resulting in uncertainty, and transfer such uncertainty into the final prediction. Geostatistics is no substitute for the geologist's experience in formulating the model properties, but it may help in creating the model. Journel (1994) accedes that geologists, at times, have become alarmed at the notion of geostatisticians treading over turf and replacing some of their well-thought-out deterministic depositional models with "random numbers." Conversely, some engineers may have been wary of geostatisticians lending their numerical skill to geoscientists to impose upon them reservoir models with resolution far beyond that of traditional and comfortable layer-cake models, a resolution whose accuracy has been questioned and which, in any case, flow simulators cannot accommodate. Such concerns should be put to rest as reservoirs modelling becomes truly interdisciplinary, and geostatistics is seen not as a self-centred discipline but as a set of tools to be used jointly by geologists, geophysicists, and reservoir engineers (Journel 1994). Webster and Oliver (2007), Chambers et al. (1994) states that the environment is continuous. However, it is possible to determine its properties at a particular point of places at any time. Somewhere else, the best that could be done is to determine, or forecast, in a three-dimensional sense. This forms the major reason for geostatistics analysis as it permits an analyst to do deprived of unfairness and with the smallest error. This allows dealing with properties that differ in dimensions that are far from systematic and at all spatial scales. Moreover, another additional feature of the thing of interest is that at some scale, the values of its properties are positively related (statistically and physically related). Places and locations close to one another tend to have similar values, whereas ones that are farther apart differ more on average. This intuitive knowledge of lateral

variation is what geostatistics expresses quantitatively and then uses it for prediction. Inevitably there is an error in estimates, but by quantifying the spatial autocorrelation at the scale of interest, errors can be minimised and also estimated. Geostatistics is also very capable of handling questions of the probability of occurrence of properties at locations at certain proportions. The era of building single best reservoir models from seismic and well logs is passing because a single deterministic model cannot capture seismic and geologic uncertainties (Caers et al. 2003). Deterministic models, generated at the scale of the seismic data, neglect any small-scale geologic heterogeneity that may have a major impact on reservoir flow performance (Robinson 2001). The resulting high resolution (both vertical and horizontal) 3D volume is well suited for use in building detailed property models. The impedance realisations from stochastic inversion can then be used to estimate the uncertainty in reservoir property such as lithology or porosity in the form of probability maps and volumetric uncertainty. The realisations can also be used to estimate reservoir connectivity and associated connected or swept volume uncertainty (Frykman and Deutsh 2002), Strebelle (2001); Liu et al. (2004); Hoffman and Caers (2005).

The study characterises the reservoir "P" field by integrating a suite of wireline log and 3-dimension seismic data volume in the study area. Numerous diverse techniques such as geostatistical methods using conditional sequential Gaussian simulation and multi-layer perceptron neural network, and approach which combines seismic inversions and multi-attribute transform, were utilised towards the accomplishment of the purpose of the study in "P" field, Niger-Delta.

1.1. Location and geological framework of the study area

The studied area (P field) lies in the Niger Delta petroliferous basin, a productive hydrocarbon area in the Gulf of Guinea, southern Nigeria. The northern part of the boundary at 300,000 km^2 Niger Delta Province is the Benin flank- an east-northeast trending hinge line south of the West Africa basement massif. Outcrops of the Cretaceous on the Abakaliki High define the northeastern boundary. The east-southeast edge is outlined by the Calabar flank- a hinge line bordering the adjacent Precambrian. The area of study is covering an area of 55 km^2. The cross-lines and in-lines are in the ranges of1480 to 1700 and 5800 to 6200, respectively (Figure 1). The Niger Delta oil and gas province is situated in the Gulf of Guinea on the west coast of Central Africa (Figure 2) After Damuth (1994), and extends entirely over the Niger Delta zone (Stacher 1995). The Niger Delta consists of a generally regressive clastic succession that is 10–12 km thick. The field comprises a single recognised petroleum system, which is the Tertiary Akata-Agbada petroleum system. While the boundaries of the province coincide with the maximum extent of the system, the minimum petroleum system is well-defined by oil and gas field centre points. The Tertiary classification of Niger Delta is subdivided into three large stratigraphic parts (Figure 3): Akata, Agbada, and Benin Formations in the downward direction of sedimentation. The basinward decrease in age is a reflection of the overall regression of environments of deposition within the Niger Delta clastic wedge province. These Formations show a massive coarsening-upward progradational clastic wedge (Short and Stauble 1967) deposited in fluvial, deltaic, and marine environments (Weber 1986; Weber and Daukoru 1975). Akata Formation: This formation is of marine origin and comprises predominantly of over-pressured, under-compacted shales of the pro-delta facies. Other lithologies that are present include insignificant amounts of silt, clay, and turbidite sand. Short and Stauble 1967, described this type of section of the Akata Formation in Akata well-1, 8000m east away from Port Harcourt. The thickness of the Formation is appraised to be 21,000 feet thick in the central portion of the clastic wedge. The lithologies, probably of the turbidite flow origin, are silts and dark grey shales with occasional streaks of sand. The oldness of the Akata Formation is between Palaeocene to Recent. It was formed during low stands when terrestrial organic matter and clay were transported to deep water areas characterised by oxygen deficiency and small energy circumstances. Agbada Formation: The deposition of the Agbada Formation began in the Eocene and continues into the Recent. The formation consists of paralic siliciclastics over 3700 metres thick and signifies the definite deltaic percentage of the sequence. The depositional environments include fluvial-deltaic, delta-topset, and delta-front systems. The Agbada Formation overlies Akata lithostratigraphic unit. Shale and sandstone beds were deposited in equal proportions in the lower Agbada Formation; though, the upper portion has minor shale interbeds with mostly sand. The Agbada Formation is defined in the Agbada well-2, drilled about 11 km north-northwest of Port Harcourt (Short and Stauble 1967). The well had a total depth of 9500 feet and did not penetrate the base of the formation. The sand layers of the Agbada Formation bear saline water. Considerable difficulties came-up with the delineation of the bottom and top of the Agbada Formation (Figure 4). Benin Formation: The Agbada Formation is overlain by the third formation, the Benin Formation, a continental deposit of alluvial and upper coastal plain sands that are up to 2000 m thick (Avbovbo 1978). The type section is Elele 1 well, drilled about 38 km north-northwest of Port

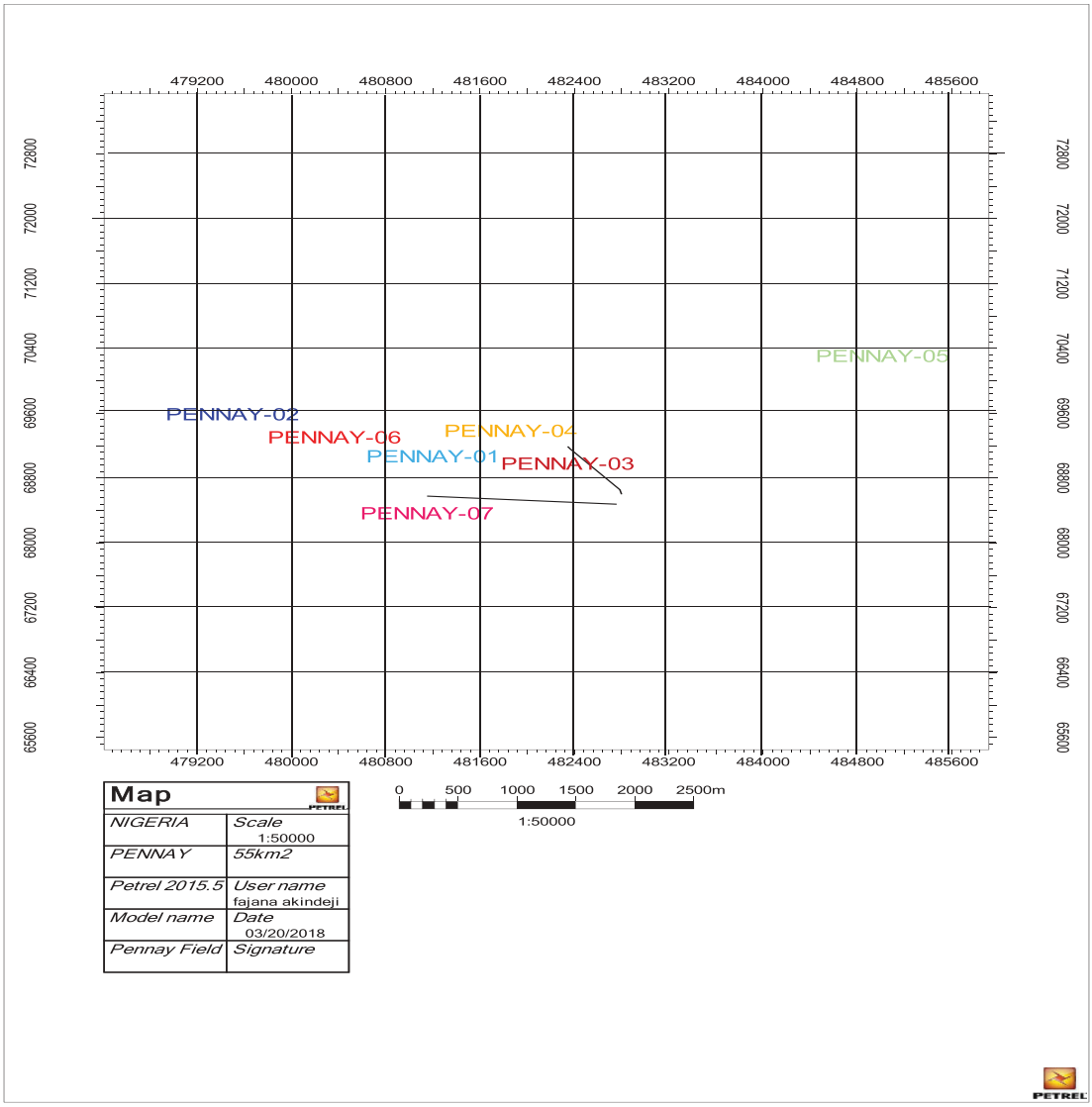

Figure 1. Base map of the study area.

Harcourt (Short and Stauble, 1967). The youngest marine shale defines the base of the formation. The age of the Benin Formation is from Oligocene to Recent. The continental sands of this formation bear freshwater.

The lithostratigraphic units constituting the Niger Delta are derived from surface and subsurface data. Sedimentation in the Niger Delta was favoured by the rate of deposition, which was higher than that of subsidence. Sediments that were supplied to the delta by Niger, Benue, and Cross-River, which acted as the drainage system. The sedimentary sequence of the southern Nigerian basins has the origin divided into three main tectonic phases, coupled with transgressive and regressive movements of the ancient sea.

1.2. Hydrocarbon potential and traping mechanism of the Niger Delta

Hydrocarbon Potential: The most useful source rocks probably are shales interbedded with deltaic sands in the lower part of the paralic sequence, and shales in the upper part of the marine sequence. The lower part of the marine sequence may contain good source rocks as well, but oil generated from this section would have to surmount long vertical migration path to reach the overlying reservoirs. The Niger Delta holds enormous petroleum reserves estimated at 30 billion barrels of oil currently 260 trillion cubits feet of natural gas. It ranks seventh in the world production and averages now about 1.8 billion bbl of oil per day (BP 2014). The Benin Formation, though mostly unaffected by gravity tectonics, has been subjected to a regional tilting southward as a result of down-dip subsidence along the fault detected. Agbada Formation is the most deformed and, as such, traps most of the hydrocarbon that has been found hitherto. Oil found in the Agbada Formation is of the paraffin type with deficient Sulphur and asphaltic cement.

Trapping Mechanisms: A trap is a geological feature of a reservoir, which is capable of barring oil and gas from moving. A closed structure in porous

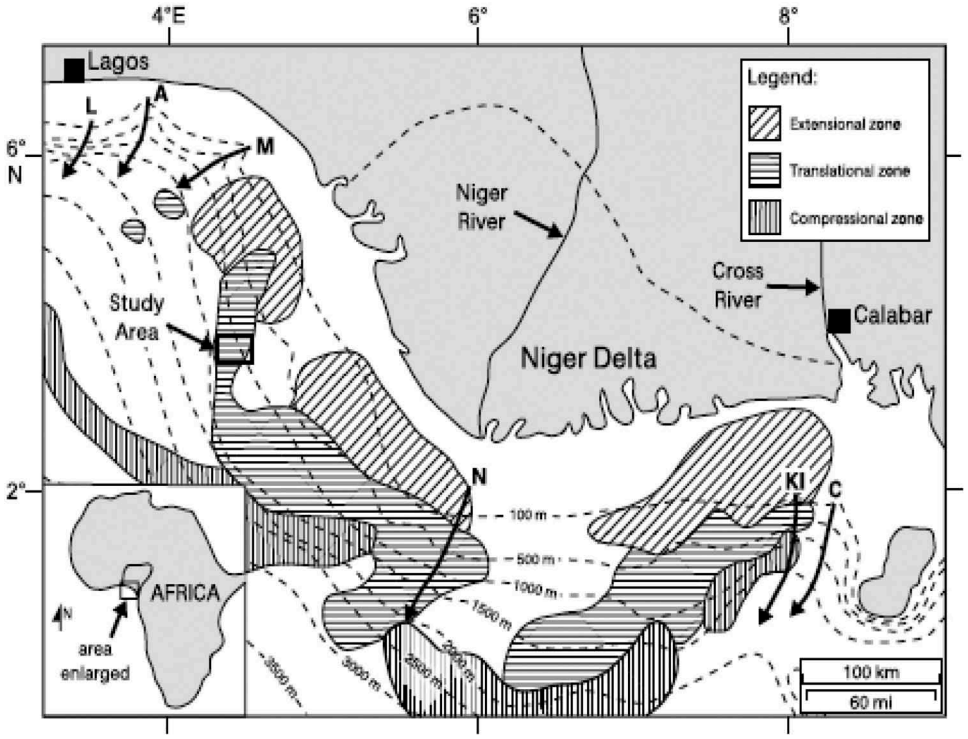

Figure 2. The Niger Delta continental margin showing bathymetry, zones of gravity tectonic and structural style (After Damuth 1994).

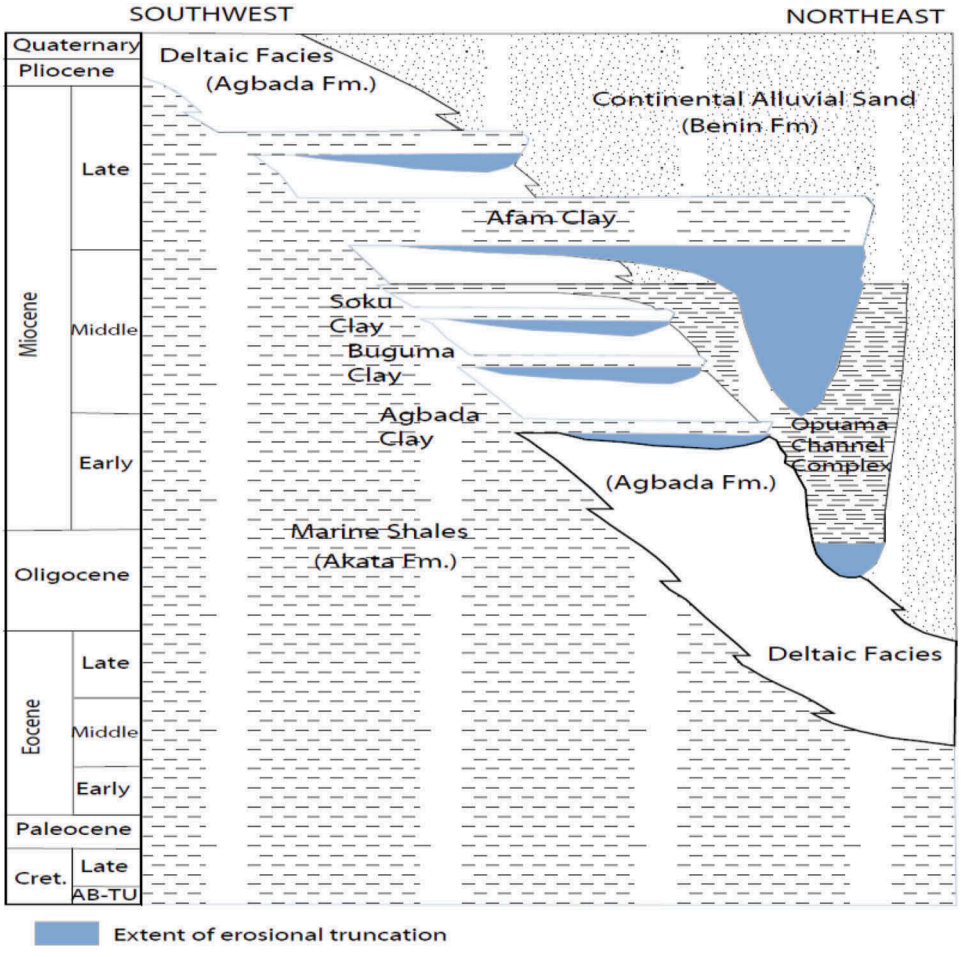

Figure 3. Stratigraphic column of the three formations of in Niger Delta. (Shannon and Naylor 1989).

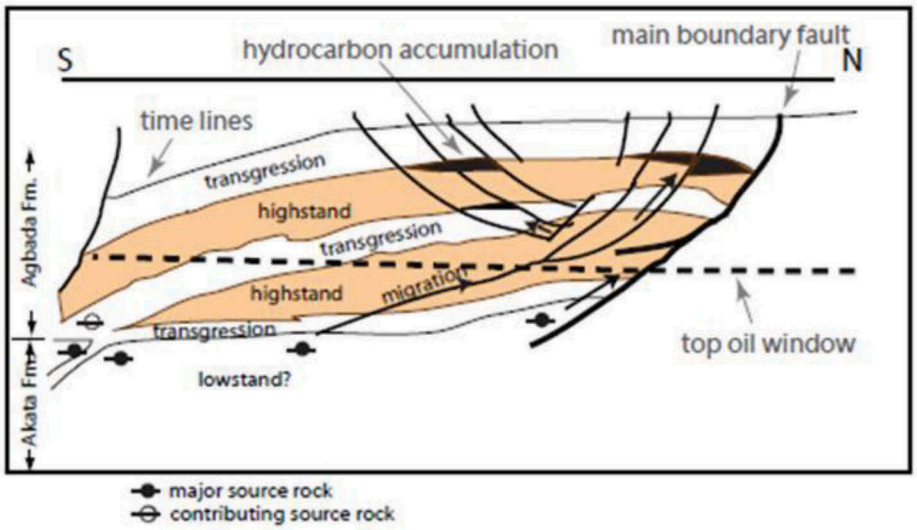

Figure 4. Hydrocarbon traps, source rock and migration pathways and associated with growth faults in Niger Delta (After Stacher 1995).

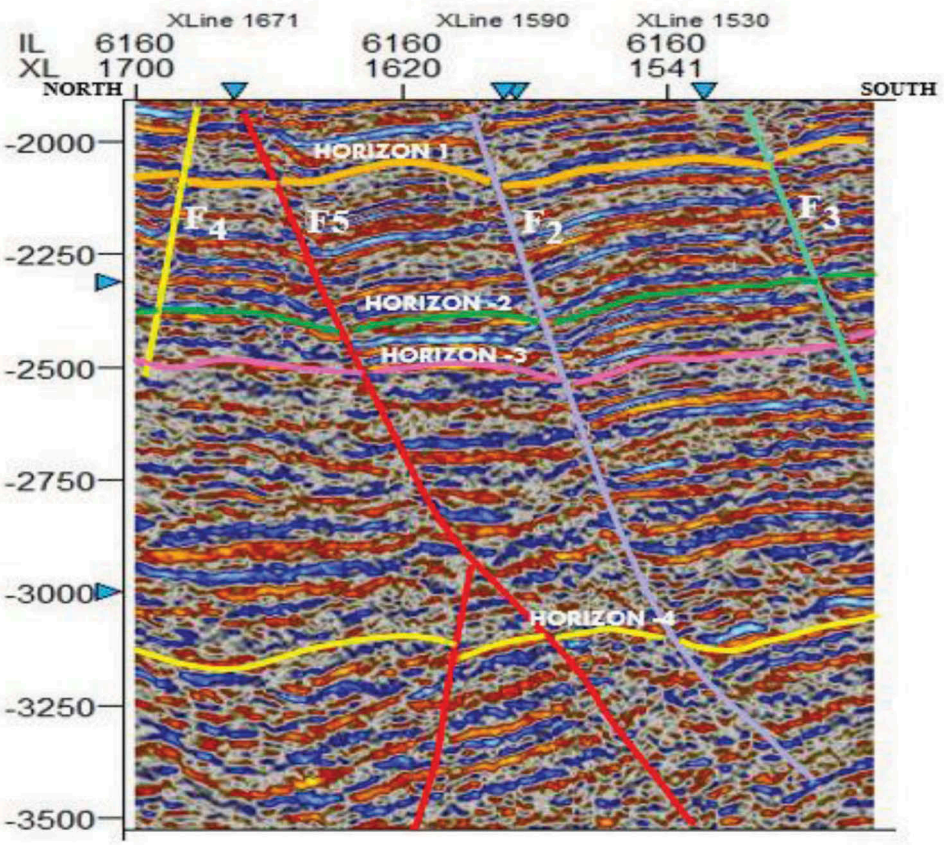

Figure 5. Typical interpreted seismic section (Inline 6190).

formations may be a trap if it has an impermeable cap rock in an enclosed structure. It may also be a trap if permeability variation block off the escape route of fluids. The hydrocarbon moves through the water both laterally and vertically until it is barred from movement by an impervious rock layer. In the Niger Delta, hydrocarbons are dominantly trapped by rollover anticline and fault closure (Evamy et al. 1978). The traps found in the Niger Delta can be grouped into three broad types, namely: Structural traps, Stratigraphic traps, and Combination traps.

Structural Traps: Most of the hydrocarbon traps of the Niger Delta are structural traps and where developed as a result of syn-sedimentary structural deformation in the Niger Delta. It has given rise to a variety of growth faults, rollover-related features separated by regional dipping flanks. Common structural traps in the Niger Delta are: (i) Unfaulted rollover anticline,

(ii) Multiple or synthetic fault closures, (iii)Anticline or synthetic fault closures, and (iv) Collapsed crest structures.

Stratigraphic Trap: The stratigraphic trap occurs as a result of lateral changes in the lithology of reservoir rocks. They are formed when permeable bed grades into an impermeable bed, as might result when sanding grades into shale. This is due to the environmental conditions at the time of deposition. The original deposition of the strata may control these variations as in the case of a channel or reef bar. A stratigraphic trap has been defined as the one in which the chief trap making element varies in some of the stratigraphic or lithology or both of the reservoir rock as facies changes, Variable local porosity, or an up-structure termination of the reservoir rock.

Combination Traps: These traps are made up of a combination of two or more mechanisms. Both the structural stratigraphic elements form them. They occur when the reservoir rock has folded into an anticline and subsequently partly eroded and sealed by the deposition of shale above the unconformity. Examples are salt domes-overlying domes and fault: salt dome cap rock and compaction anticline.

1.3. Datasets and methodology

The methodology adopted for this study was based on the data set available. It starts with conventional well logs analysis, computations of rocks petrophysical properties, clustering analysis for lithofacies identification, well logs normalisation, well logs upscaling, time to depth conversion, conventional seismic interpretation for horizons and fault, seismic attributes computation and analysis, model building, variogram analysis, data analysis, seismic facies, seismic inversion, seismic multi-attribute analysis, and geostatistical simulation. The following data were loaded into the project: Wellheads were imported for each of the wells, Well path/deviation data were imported for each of the wells, Well logs were imported for each of the wells, Check shot data was quality-checked and Seismic volume was imported. The sets of data accessible for the research include a volume of three-dimensional (3-D) seismic data, a base map showing inlines, crosslines and location of wells, suites of borehole log for seven (7) wells and two-way-travel time versus depth data (check shot). The 3-D seismic data volume has a dominant bandwidth of 65hz. It is a post-stack data, 58 folds, zero phases, and migrated. It consists of 201 crosslines, and 401 inlines. Gamma-ray logs were used to delineate various lithologies in the study area.

1.3.1. Clustering analysis

In this approach, available wells were used to build the model for the area. The volume of shale log (Vsh), GR log, and porosity log were used for the model because of the non-linearity effect in their cross-plot and ability to accurately resolve lithofacies distribution. The depth of investigation was selected in a sequential pattern based on the understanding of the necessary prior interpretation made on the wells. However, the model was ultimately built to cover the whole run of the wells. This is necessary to achieve one of the high aims of the entire project, which is to create a valid facie model. Having set up the input panel to suit the distribution patterns. Cluster mode or seed clusters were the initial maximum number of classes into which the observed values of the input logs were distributed before the agglomeration. The Opendtect software was used for this operation, and it was achieved by initialising the run engine in three ways; values can be typed manually into the grid, the seed cluster can be randomly assigned by allowing the machine to make the sorting and thirdly, the cross-plot button on the cross-plot display can be used to move pre-assigned points interactively. In the seed cluster approach, a principal component analysis was performed on the input data, the result sorted and equally divided into the defined number of classes. From the cluster classes, the low and seed points were computed, and thus the slots were populated for each input variable. Then the clustering run was set for the program to calculate the standard deviation and mode for the classes, due to the pertinence and sensitivity of the previous step, physical examination of the distributions commenced afterwards at this point by deleting the row (the convergence clustering point values) with a small mode. This helped initiate a recalculation to optimise the analysis. The distance is a function of the value of logs used in building the clustering model. Histograms and cross plots outputted from model building assisted in physically observing the cluster groups before the secondary agglomeration to some smaller geologically plausible facies.

1.3.2. Well logs upscaling

The well logs upscaling is the blocking of well logs values into the property's coefficient within a simulation grid cell; this is done in a variety of ways. When modelling petrophysical properties, the modelled area is divided up by generating a 3D grid. Each grid cell has a single value for each property. Since grid cells are often more significant than the sample density for well logs, values that fall within the cells were averaged according to the selected algorithm to produce one log value for that cell. For discrete well logs (facies or zone logs), the conventional method of "Most" is recommended. The upscaled value then corresponds to the value which is most represented in the log for that particular cell. The layout and resolution of the 3D grid will control how

many and which cell each well penetrates. For instance, a dipping layering scheme, compared to a horizontal system, can/may alter the results from the scale-up of the well logs and the subsequent property modelling. The averaging method chosen for each type of record is a function of the nature of the logs as it relates to its character. Also, wells are treated as either points or li8nes. Eventually, the statistics and histogram of the result of the upscaling operation were checked up if there is an agreement between the raw logs and the upscaled well logs. This quality control step did not stop at this point, the understanding of the raw logs upscaled well log, and the simulated volume was visualised to see the extent of deviations and the success of the operations.

The approach that was used for well upscaling was in two parts. The first part was one that concentrated on the discrete log types. These are necessarily the facies log both from clustering operation and from the use of cut-offs through visual observations. All well logs were upscaled from the raw well logs and not from well attributes or point attributes.

This is because the cell averaging taken into consideration earlier in building the model. Well, attributes and point attributes are point properties, not a good representation of the vertical distribution of properties. The cell size was fixed at 1m and the averaging method of "Most of" was chosen and were also treated as lines so that each log sample was weighted by a factor that is proportional to its interval as the well path passes through the earlier blocked cells in the simulation case. The neighbour cell method property blocking was used that averaged the log values from all cells adjacent to the upscaled cells, and that belong to the same layer as the upscaled cell (Figures 3.9a 3.9b).

For the continuous logs, a similar approach was used, but an attempt was made to use the earlier blocked (upscaled) facies log as a biased estimator for cell population for some petrophysical records, like porosity. The use of estimation bias did not quite work well on continuous logs. This is because of the nature of log (i.e., combination flaw – discrete and continuous data). Well-Logs with more straightforward (e.g., GR and Res) physiochemical theoretical basis was scaled up using the arithmetic and harmonic averaging method. This was done in a way to account for the seeming heterogeneity noticed in the well logs analysis done, and also the anisotropy evident in lateral reconciliation of similar rock properties.

1.3.3. Seismic inversion

All inversion and multi-attribute volume prediction were done in the Opendtect Pro 6.2 software. Seven (7) well logs and 3D seismic data volume were used for volume inversion operation. The wells had logs with proper signatures and were at random locations on the field. The primary treatment on the logs was to correct for spurious frequency and static shifts based on check-shots. Four (4) Horizons that were previously picked from the initial workflow from Petrel were imported into the software (petrel and Opendtect). A vintage seismic volume was imported for use in the inversion program. After correcting the well logs, trace extraction was done to correlate the well logs with seismic trace. To achieve this, a composite trace extracted around the wellbore was required. The neighbourhood method was used for the composite trace extraction around the borehole. This step was used to optimise time-depth conversion. The next step was to extract a statistical wavelet having an initial zero phase, which has an amplitude spectrum derived from raw seismic before correlation at different stages. After obtaining the statistical wavelet, the synthetic trace was shifted to match the character of the natural seismic and composite traces. After achieving a good correlation, another wavelet was extracted this time from the wells that were being correlated to confirm the validity of the operation, and also, a multi-well analysis was done to see how the wavelet behaves across the spread of the locations where there are wells. The model-based algorithm was employed, and the method is deterministic. The model was built around the wells and horizons present. The neutron, sonic, and density logs present on the wells were used in the P impedance equation. Because seismic data lacks the low-frequency component of the rocks, and a correct interpolation of this frequency around the volume from the logs was desired, and a high cut frequency filter was applied for this method. It was worthy of note that the model adopted was constrained to field geology by the horizons initially interpreted (Figure 5).

Sequel to model building, an analysis was done in two stages. First, the investigation was run at well locations to optimise the modelling parameters, and then the whole volume was treated to the parameters chosen in the first step. This was the analysis of the inversion model before the actual volume inversion. Here the time or analysis window, the target zone, the composite trace extraction method, and the scaling factor were set. The inversion operation was done after proper analysis. The procedure adopted raw seismic sampling rate, average block size – 4ms as in sampling rate above, pre-whitening –1%, number of iterations – 10, and infinitesimal spuriousness.

1.3.4. Multi-attribute volume prediction

This is an aspect of the workflow that strives to predict volumes of subsurface rock properties from the vintage raw seismic initially alone subjecting it to multi-attribute analysis after attribute sensitivity analysis had been carried out And subsequently inculcating the predicted volumes as an external attribute to be added to the suite of multi-attributes used for some

other volume predictions. Well-logs and seismic data were imported. The purpose of this was to predict well log properties at points where it does not exist using seismic data. The analysis progresses from the primary examination of the log and seismic data at well locations to determine which set of attributes was appropriate, and then a relationship was derived using multi-linear regression or multilayer perceptron Neural Networks. The defined relationship was now applied to 3D SEGY volume to create a volume of the desired property. Single attribute analysis was performed then followed by performing multi-attributes analysis to see the set of combined seismic attributes that best predicts the properties. The method of analysis was primarily least square regression (stepwise) analysis on the well as they correlate with logs basically to reduce uncertainty in results

output. For porosity and other petrophysical properties, a probabilistic neural network training algorithm was also used. Additional external attributes were imported to add to the prediction database and further made the result less erroneous since post-stack data was used. Volumes computed/predicted are porosity, NTG, permeability, and Hydrocarbon saturation. Having derived the best combination of attributes for each property, the best attributes set was applied to 3D volume to predict the rock property from the well-log and populate the volume. The average error for all well was viewed to see the agreement of the well logs property with the set of attributes chosen.

1.3.5. Geomodeling

The non-partitioned single zone models were made for the field of study and the delineated regions of interest, top middle, and base. The superficial grid of 60 × 50 x 1. The model includes both stratigraphic and structural elements. Cell configuration (nI x nJ x nK) = 260 x260 x400 and total number of 3D cells = 27,040,000. This serves as a receptacle into which all other operations were carried out. Seismic attributes inversion volumes and prediction results volume were resampled into the established 3-D grid model. Geostatistical analysis and inversion – Simulation algorithms and variogram models and were all run on the geomodel built for the zones. (Figure 6)

The 3-D models (Permeability, NTG, Hydrocarbon saturation, porosity, and facies) were built similarly in Petrel 2015 software, the main difference being the type of log used to populate the grid cells and the computation formulae, in deciding which wells to use in the models, and the size of the model domain needed to be established. If too big an area were selected, then there would be more space in between each well and less data control from the well logs, which could correlate to less accurate models. Thus, a reasonable zone model boundary was made to enclose the zone of interest that characterises the stratigraphic and structural elements in each portion. A smaller area would yield a smaller but more detailed model. Due to several available and useful well logs, an area measuring ~ 55km2 was covered using seven wells.

2. Reservoirs and rock properties prediction using artificial neural network

This segment of the study involves the prediction of the spatial distribution of rock and reservoir properties in the study area using Artificial Neural Networks (ANN). Several 3D seismic attributes were used to

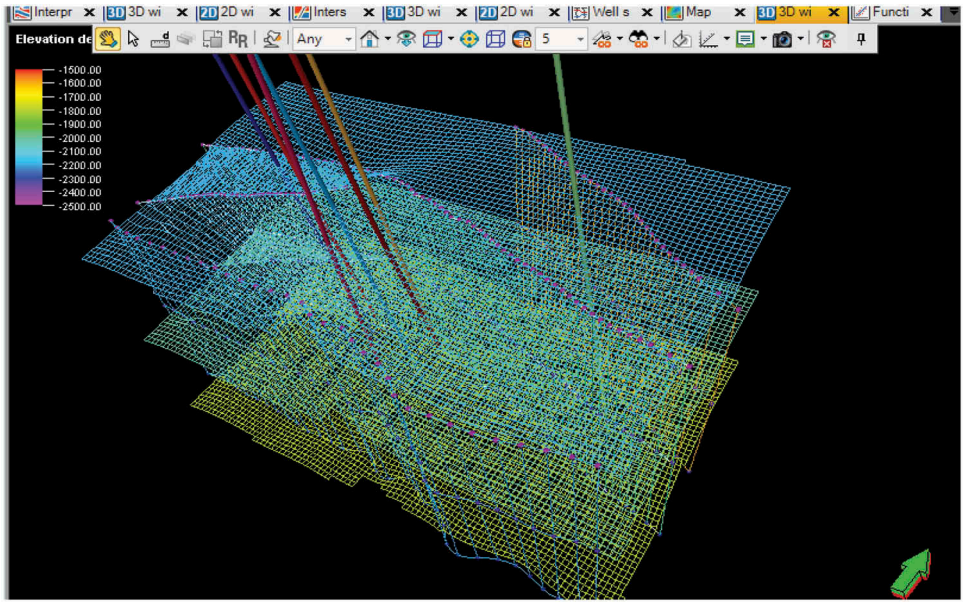

Figure 6. 3-D geomodel grid and structural framework.

predict these properties (permeability, porosity, and volume of shale and hydrocarbon saturation) away from well control. Well-to-seismic ties were considered to be the training points for the method; both the seismic response and the well log property were known at the selected well locations. A statistical relationship, either linear or nonlinear, was developed at the well sites to relate seismic response to a well log response.

This is a supervised approach using a multilayer perceptron neural network. The network found the optimal (non-linear) mapping between seismic attributes and target well log characteristics (porosity, net to gross, Volume of shale, and water saturation). The network is trained on data points extracted along the well tracks (Figures 3.22 and 3.23). Part of the extracted points was used as a test set to determine the optimal position to stop training and avoid overfitting. The trained network was applied to inverted seismic data. The input data (inverted seismic) needs to be scaled to match the scaling of the input data set that was used in training (logs). Theoretically, we only need the attribute value at the evaluation point as input to the neural network, but this assumes that the inversion process has completely removed the wavelet and that there is perfect alignment of attribute and log responses along the entire well track (Helle et al. (2001), Rafael and Reinaldo (2002). To compensate for potential inaccuracies, the Extraction of more than just the attribute value at the evaluation point was executed. An extracted attribute in a 24ms time window that slides along the well tracks was also done. Furthermore, the corresponding log values from the depth-to-time converted and resampled logs serve as target values for the neural network. The workflow is schematically shown in Figure 7

3. Results presentation and discussion

3.1. Petrophysical assessment of reservoirs

Figure 8 shows the lithostratigraphy correlation of wells in the "P" field, showing the sand and shale intercalation. The field has an average porosity of 28%, average hydrocarbon saturation of 60%, average permeability of 721md, the average volume of shale of 8%, The reservoirs were characterised by a gross thickness of 120 ft, 103 ft, 112 ft, and 115ft. Net to gross ratio is 100% in well 1, well 2,3, and well 4, respectively. The average volume of shale is 8%, which is a clear indication that the reservoirs have a large volume of the sand deposit than shale. The hydrocarbon saturation in the reservoir are 70%, 72%, 70%, 72% and 70% for "P" wells 1–5 respectively

3.2. Discussion of characteristics of sand bodies in mapped reservoirs

Low values of the gamma-ray curve observed in the reservoirs show that these reservoirs are thick

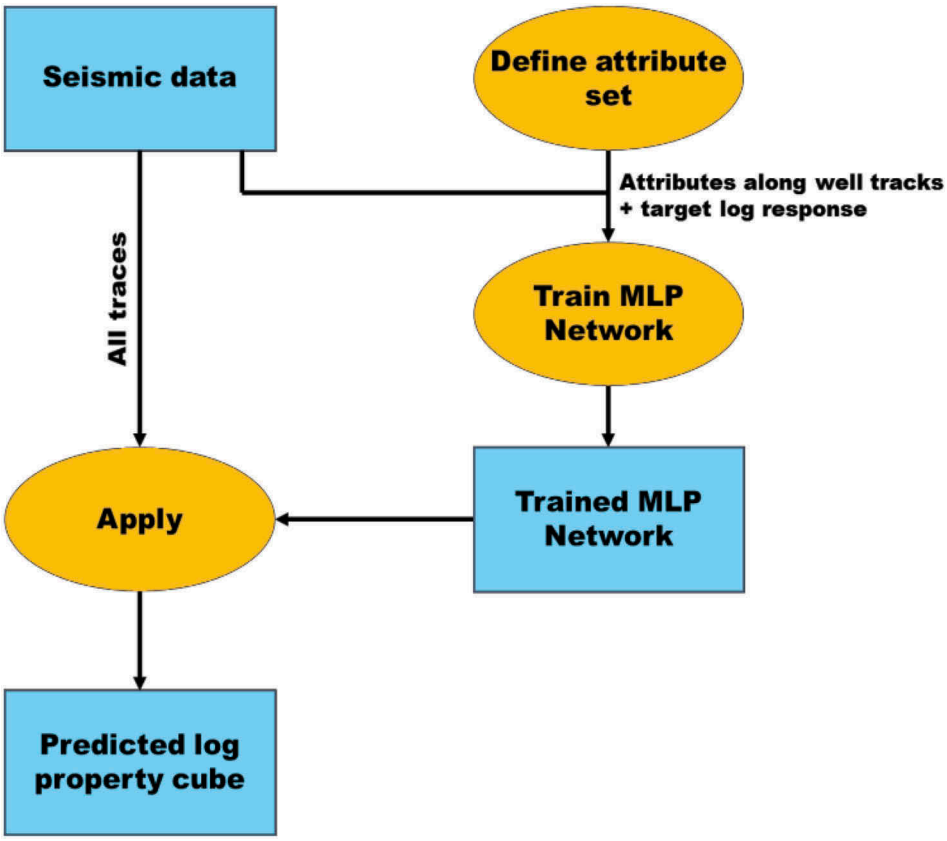

Figure 7. Log property prediction workflow using artificial neural network.

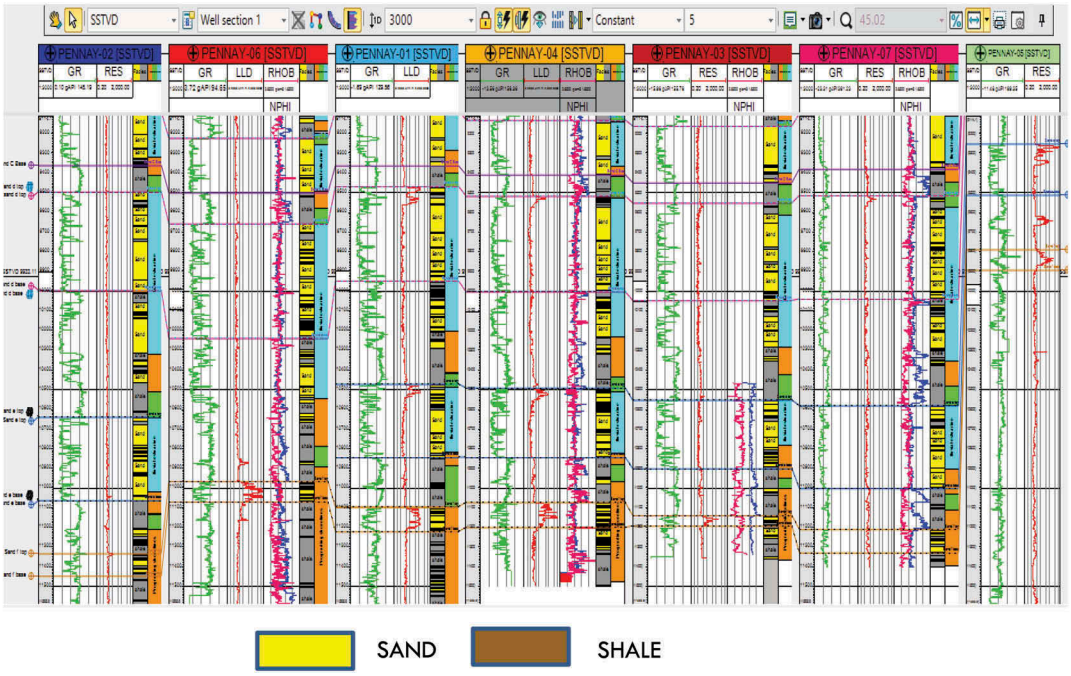

Figure 8. Depth structure map of horizon sand B.

sand-packages with shale intercalations Figure 9. The reservoirs A, B, and C have a generally blocky gamma-ray log motif. It is probably a distributary channel fill. The high value of the deep resistivity curve in the upper section of the reservoir shows that it is hydrocarbon-bearing. well-01 and 04 encountered gas – oil and oil-water- contacts (G O C and O W C) at −10524ft and −10550ft

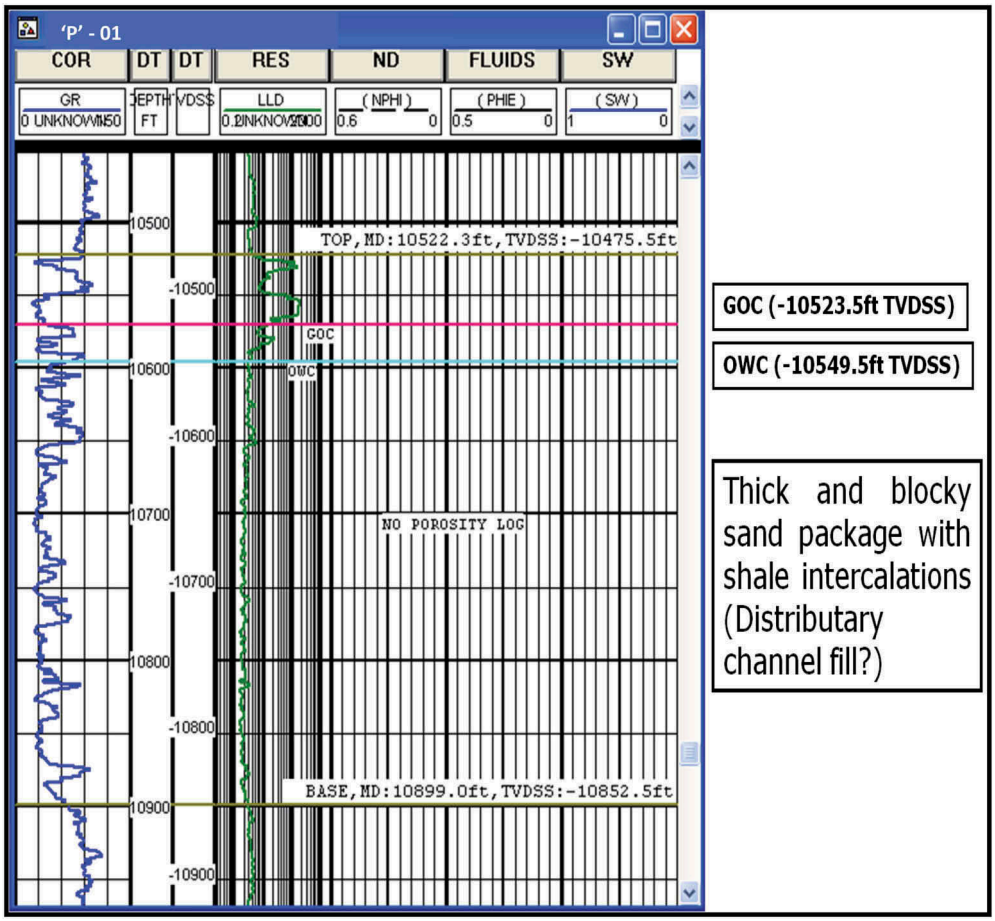

Figure 9. Log curves of "P" −01 showing reservoir C-sand.

TVDSS, respectively. The relatively low density and neutron values in this reservoir point to the presence of gas (Figure 10). In the oil pay zone, density and neutron curves track, and their values cluster around the sandstone matrix line on the neutron-density cross-plot (Figure 10). Figures 11 and 12 show a typical RMS amplitude map and fluid contact map of reservoir 2, respectively revealing regions of interest.

3.3. Seismic structural analysis

Three (3) major growth faults, F_2, F_3, and F_5, which are normal, listric concave in nature), two antithetic (F_1 and F_4) were identified. Delineated structural closures identified as rollover anticlines and displayed on the time/depth structure maps; suggest probable hydrocarbon accumulation at the upthrown side of the fault F4. Structural time maps where values are in two-way seismic travel time were generated for the mapped horizons using fault polygons, boundary polygons, and the interpreted horizon, as shown in Figure 13. Structural depth maps were also produced, and they show the exact position of structures and fault within the study area for the mapped horizons corresponding to the time-depth plot (Figures 14, 15 and 16). The crest of the structure is structurally high; hence it is a hydrocarbon prospect. It can be observed that the existing wells are situated close to and on the flank of the mapped structural high. This also confirms the validity of the previous interpretation.

3.4. Conditional simulation of rock and reservoir properties

The conditional simulation technique, conditioned by prior information, is a procedure that simulates various attributes or petrophysical property of interest at unsampled locations. These techniques constitute a part of a broader class of simulation techniques and are called Monte Carlo simulations. In this study, the sequential indicator simulation algorithm and sequential Gaussian simulation (SGS) were used in populating for the facies modelling grids and reservoir properties of the zones, respectively.

3.5. Facies model results

Facies modelling is also very vital in reservoir characterisation. It is used for simulating the sand bodies in the formation. The delineated reservoirs are composed mainly of sand and some amount of shale content. The facies models for a conventional reservoir, reservoir two (2) is shown in Figure 17. The sequential indicator simulation algorithm used for the facies modelling resulted in an adequate distribution of sand and shale facies taking control from the wellbore axis and gently spreading its influence

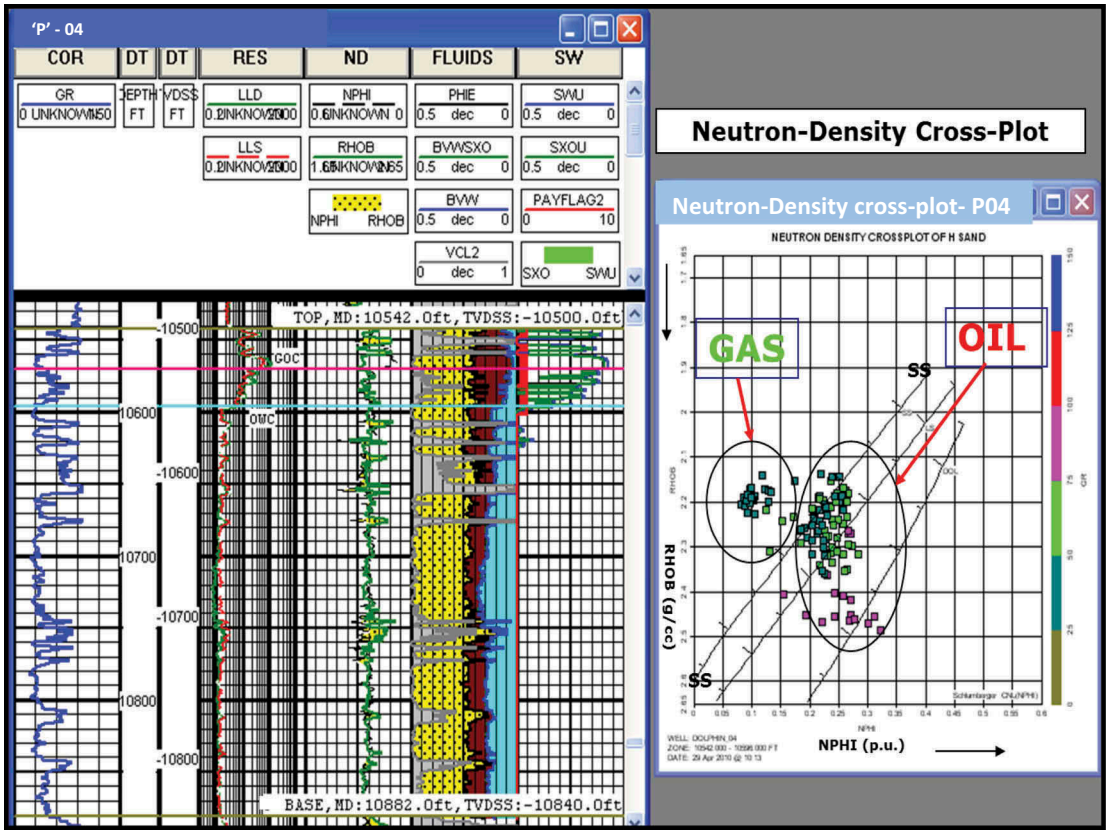

Figure 10. Log curves of "P" –04 showing reservoir C-sand and the corresponding neutron-density cross-plot.

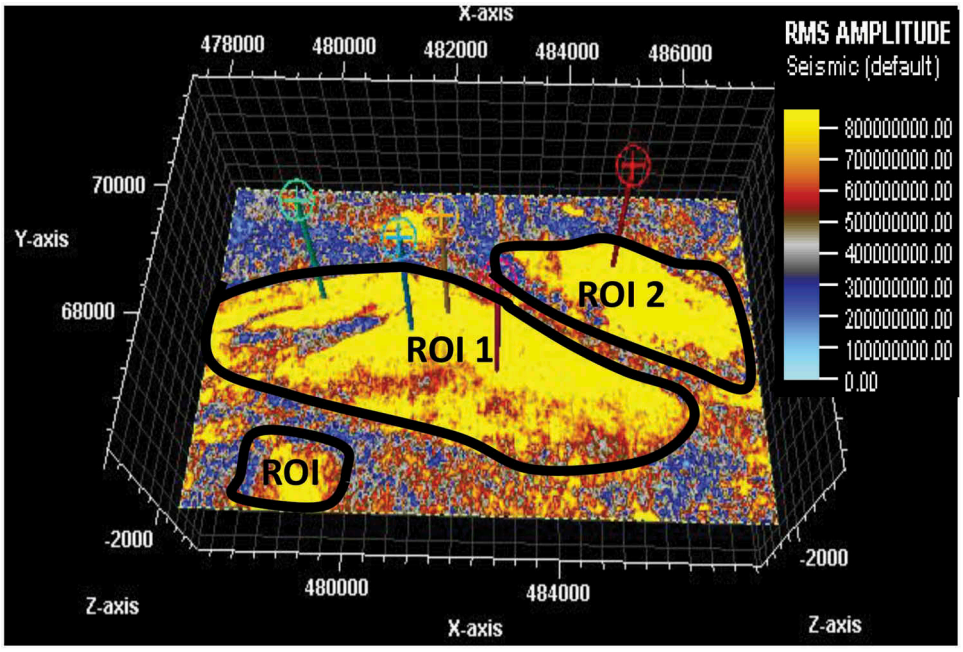

Figure 11. RMS amplitude map of top of "P" horizon 2 showing regions of interest.

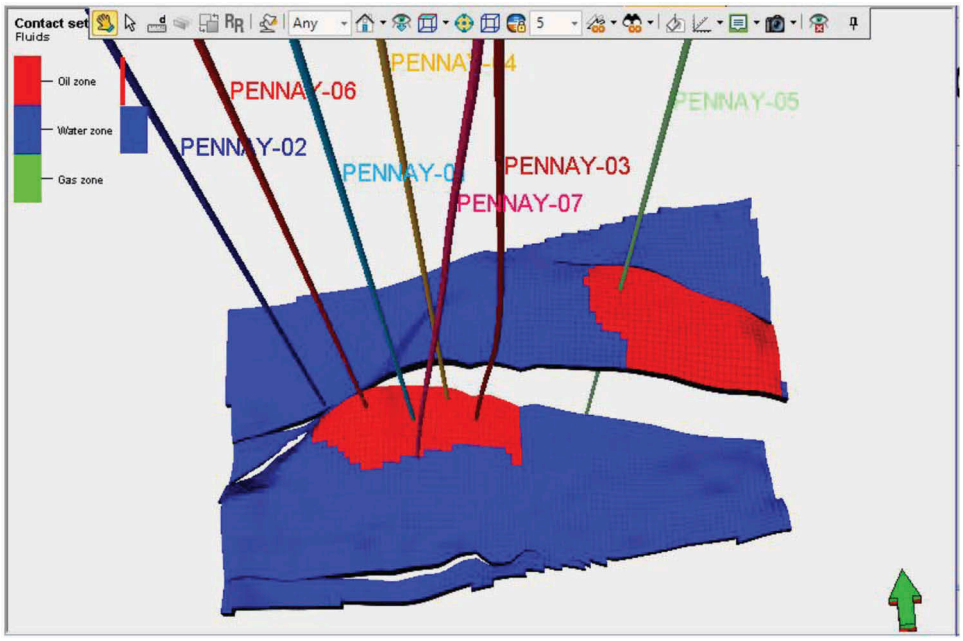

Figure 12. Fluid contact map of reservoir 2 sand unit.

across according to the semi-variance/autocorrelation parameter used in the variogram modelling. The models show the distribution of sand (yellow) and shale (grey colour) lithology within the reservoirs. The sand is more dominant in the reservoirs. There are advantages and disadvantages to the choice of model boundary used. The non-partitioned model adopted for the simulations allowed the operations (algorithm, variogram, sequential simulation) to assign facies values with the most freedom. No interior restraints are present to force facies assignments, so the full range of interpretation based on the variogram is displayed as all model elements are also inculcated. Possible misallocated cell assignments have been adequately taken care of when the variogram model is well made. The uncertainty analysis is included in the horizon making process; thus, ten (10) equiprobable realisations of different scenarios of the zone properties are obtained for each of the mapped reservoirs. The realisations were ranked based on their closeness of the actual value of a petrophysical property of interest at well locations.

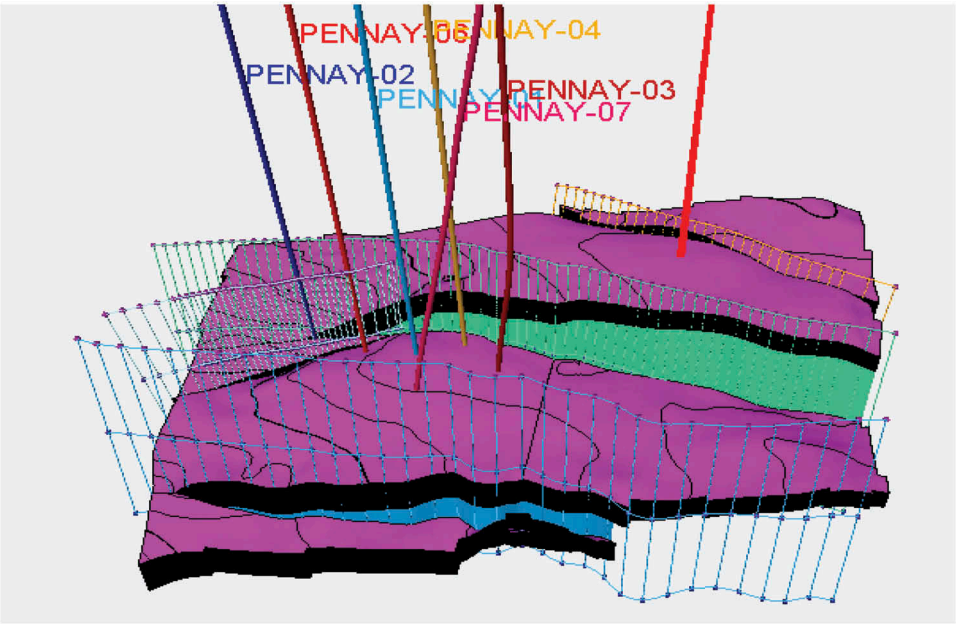

Figure 13. Fault polygon framework in the study area.

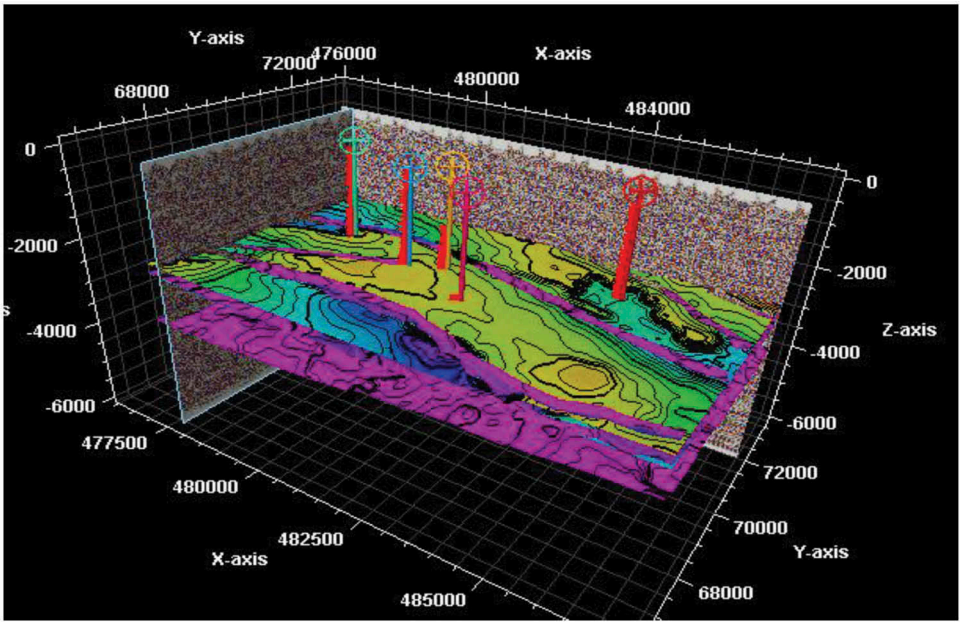

Figure 14. 3-D view of depth structural map of "P" horizons.

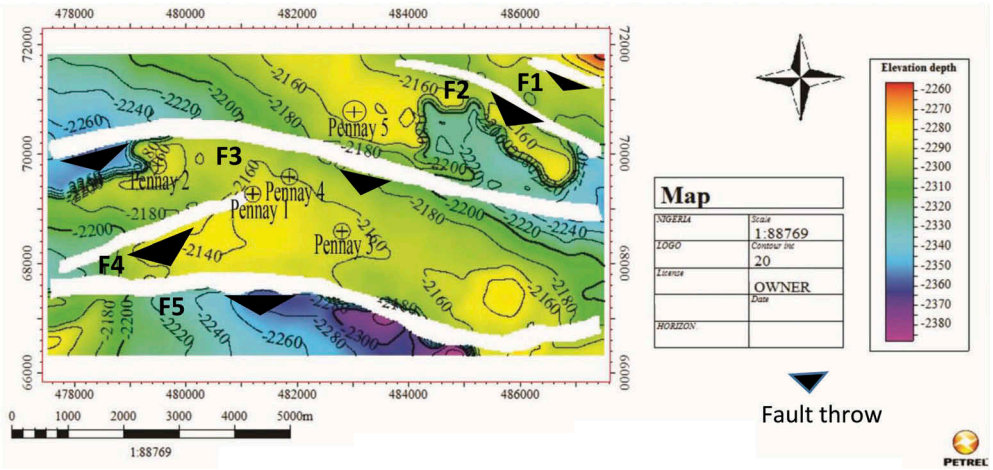

Figure 15. Depth structure map of horizon sand A.

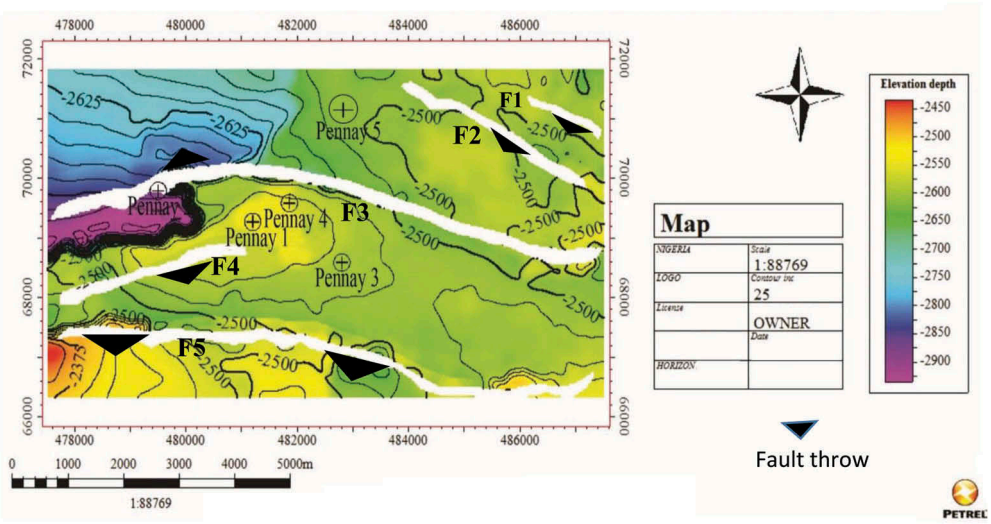

Figure 16. Depth structure map of horizon sand B.

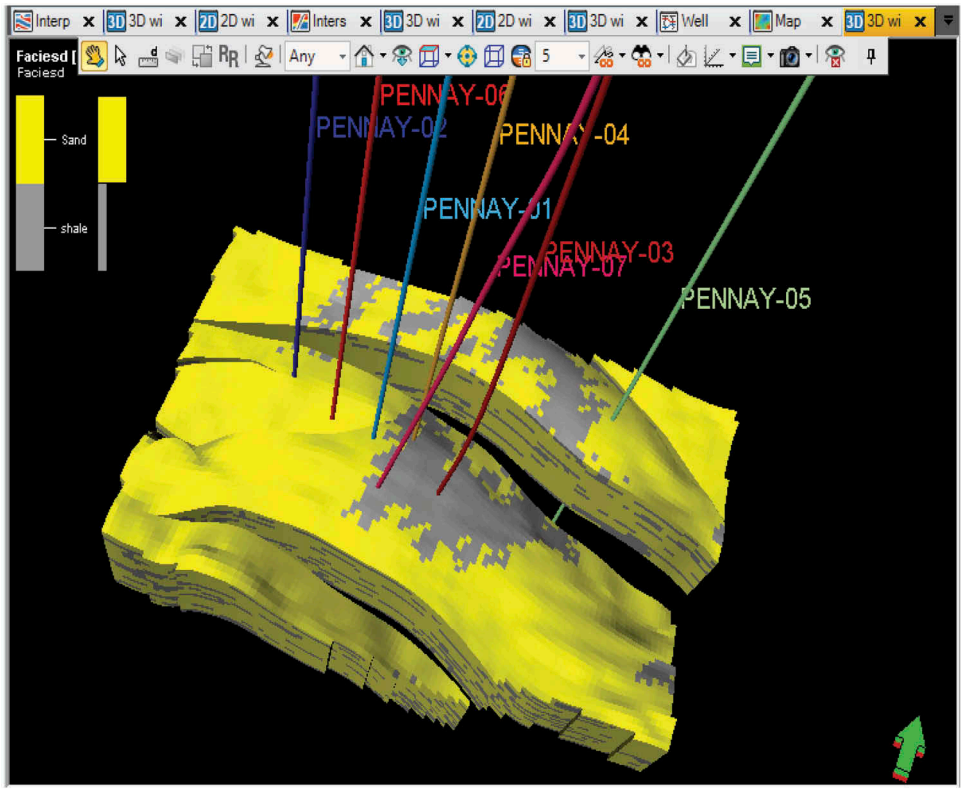

Figure 17. Sand 2 Facie modelling.

Figure 4. was rated best out of the ten (10) realisations for reservoir 2. Continuity and truncations of lithological units are seen in this Figure.

3.6. Reservoir property model results

For the continuous logs up-scaled into the simulation case, the Sequential Gaussian Simulation (SGS) was used in populating the grids for reservoir properties of the zones. The variogram for each reservoir properties made with proper consideration given to the range and sill of each log brought out the uniqueness of spatial distribution of these petrophysical properties. This resulted from single run variogram modelling, unlike the facies variogram, which was done on each facies separately before carrying out a combined simulation.

3.7. Effective porosity modelling

Effective Porosity is one of the primary parameters used for evaluating the amount of hydrocarbon in a reservoir. The computed average effective porosity from the seven (7) wells were used to estimate the porosity at unsampled

locations, and the results were distributed into the 3-D grid for a property (Figure 18). The dominant effective porosity values range from 27% – 29% (light blue to yellow colours). On observation, it was noticed that the porosity is evenly distributed within the study area. It was seen that the more significant portion of porosity property value was useful as a reservoir indicator, and it was also discovered to be in the range of value for average effective porosity derived from the logs for the mapped reservoirs, thus making the realisations reliable. Based on Conditional Sequential Gaussian Simulation algorithms, ten realisations were generated in mapping the reservoirs lateral and vertical effective porosity distributions. Visual observation shows that the models are similar in terms of distribution variability. The similarity of statistics of the models suggests that any one of the realisations can independently represent the real picture of the subsurface geology within the study area in terms of effective porosity distribution. The outputs are a set of probabilistic models that can serve as a measure of uncertainty in predicting facies distribution within the study area. Relative high effective porosity is observed in the regions of interest in the mapped reservoirs. Figure 10 was ranked best out of the ten (10) realisations in the mapped reservoir 2. There are evident of continuity and lateral variations of effective porosity within these lithological units

3.8. Permeability modelling

Permeability is also essential for reservoir rock characterisation, which is also a measure of the ability of a formation to transmit fluids. The permeability computed from the logs for each of the reservoirs were used to simulate the values at unsampled locations and was distributed across the 3-D grids. The permeability variation within the reservoirs and across fault blocks has been observed, and the permeability values modelled for the zone in reservoir 2 is 710md (Figure 19). This is as delineated within the fault truncated fairly continuous lithological units of the zones. The calculated permeability for the four (4) reservoirs ranges from 5000mD – 915mD. From the realisations, the best-ranked realisation has an average permeability of 832mD for reservoir 2. The regions of interest with relatively higher permeability coincides with areas with higher effective porosity modelled zones in the field. The models underscore ethical permeability values. The values are reflective of good interconnectivity of pore spaces of the sand within the reservoirs and well area and their ability to transmit fluids. On the contrary, the region farther away from the well locations in the south-west area of the "P" field indicates poor to good permeability, which ranges from 1 mD to 10 mD on all the permeability models.

3.9. Net to gross ratio modelling

Net-to-gross (NTG) ratio modelling was carried out to see the areal distribution of the volume of sand units within the reservoirs in the study area and determine their quality as a potential reservoir. The net to gross ratio model for reservoirs two is shown in Figure 20. High NTG value connotes a good quality hydrocarbon reservoir. Figure 4 reveals useful net to gross, which falls between 0.8 and 1 within the wells concentrated area of the field while the region farther away from the location

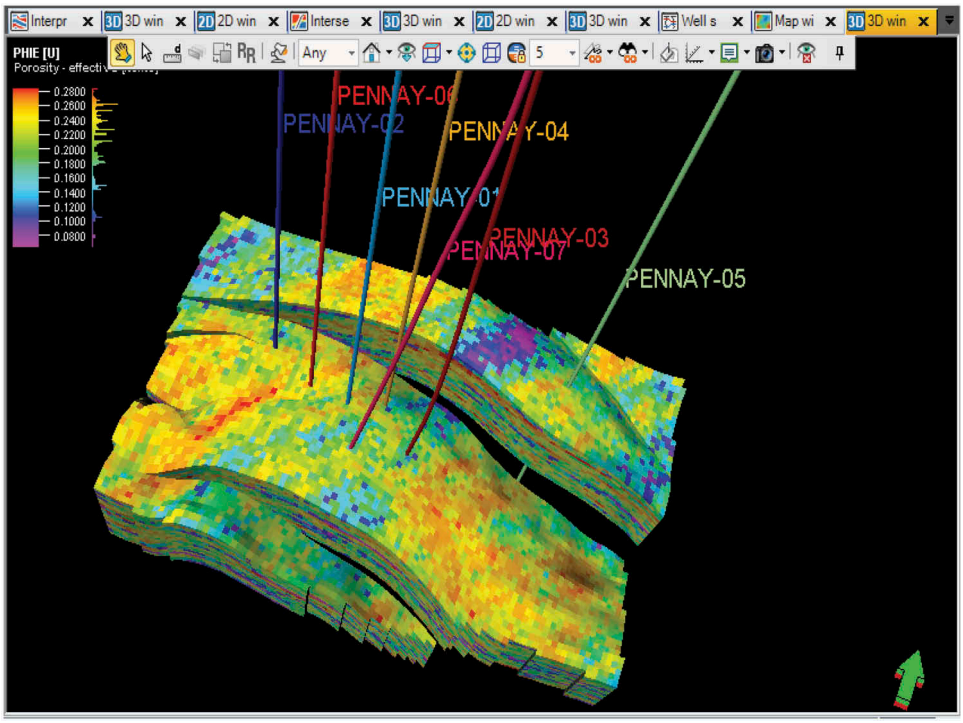

Figure 18. Porosity modelling of reservoir 2.

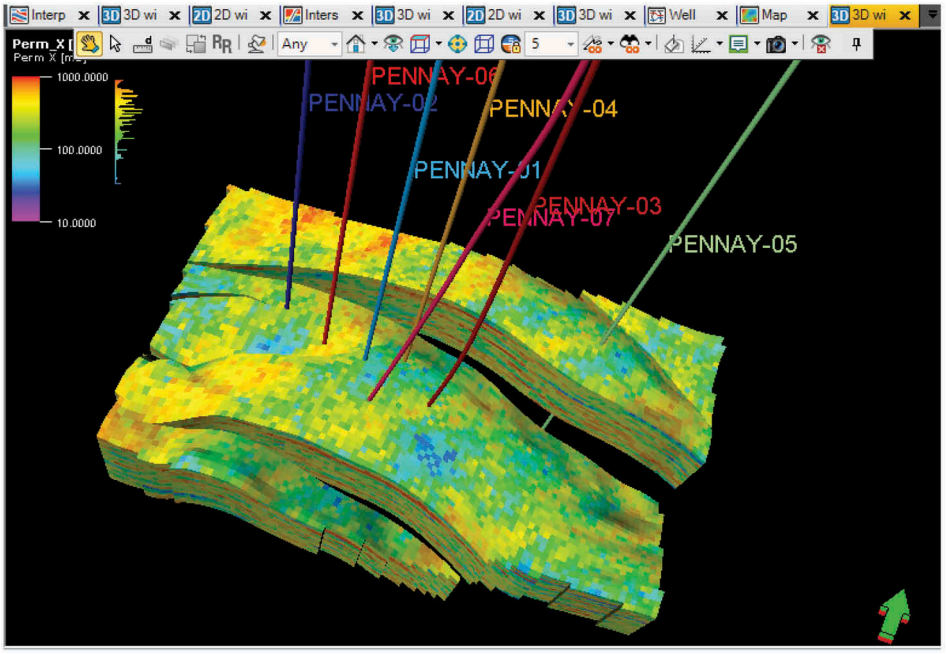

Figure 19. Permeability modelling of reservoir 2.

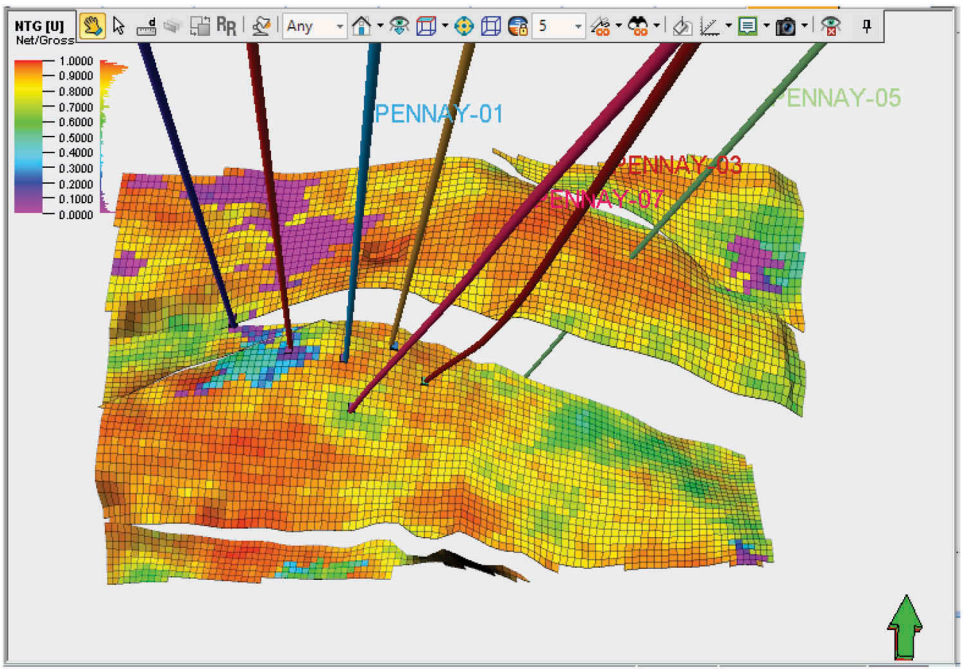

Figure 20. Reservoir 2 Net-to-Gross.

of the well is indicative of relatively low net to gross, which oscillates between 0.5 and 0.7. The sand formations are mostly continuous as it was also observed on other properties modelled, thereby confirming a high level of homogeneous nature of the zones.

3.10. Water saturation modelling

The hydrocarbon saturation is a function of the water saturation (S_h = 1- S_w). The water saturation computed from the resistivity logs for each of the wells was used to estimate the values at unsampled locations and was distributed across the 3-D grids (Figures 21(a, b)). The calculated water saturation for the four (4) reservoirs ranges from 0.23–0.57. The average water saturation is about 29% – 41%. The water saturation is uniformly distributed, like effective porosity in the reservoirs. The zones with low values between 0–0.38 (yellow and green banded colours) are of interest because they indicate regions of relatively very low water saturation, which implies a high hydrocarbon saturation in these regions. The regions of interest have excellent

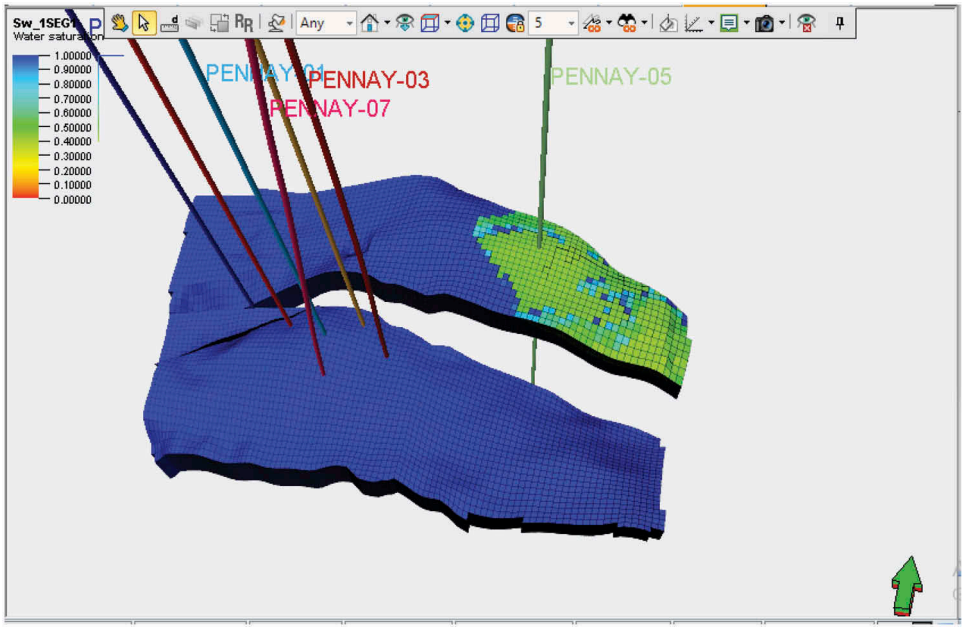

Figure 21. (a) Water saturation of the Upper part of the field in the upthrown part of the structure building fault.

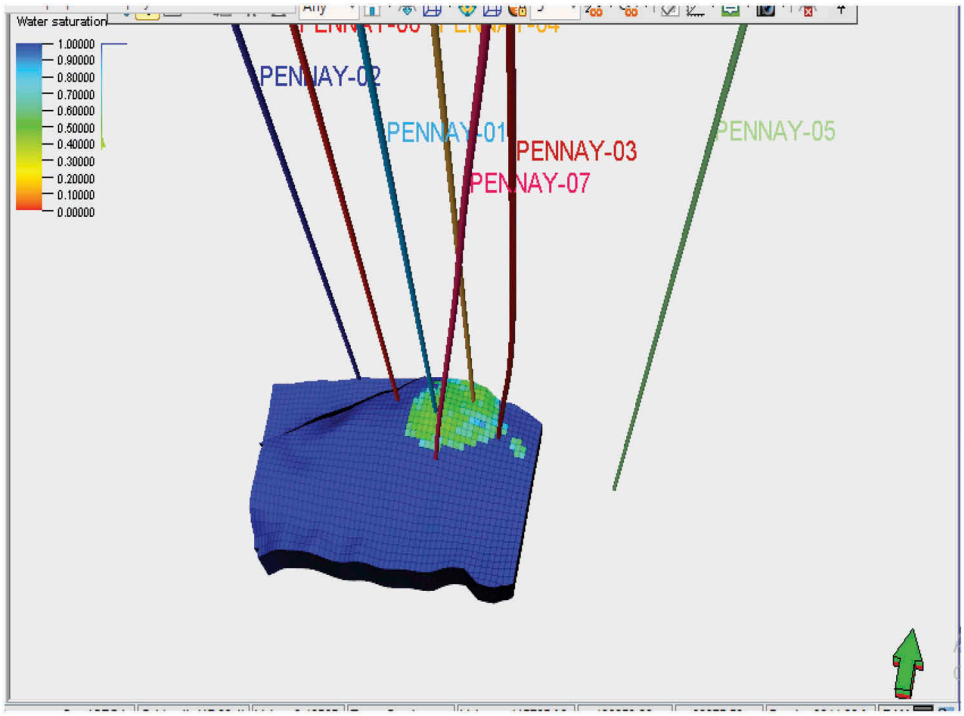

Figure 21. (b) Water saturation of the lower part of the field in the downthrown part of the structure building fault.

hydrocarbon saturation in areas with good concentration and in the northern parts of the field, which constitute the region of interest two from all models across the reservoirs.

4. Quantification of uncertainty in realisations

Quantification of uncertainty is dependent on the type of problem at hand and simulation methodology. When defining uncertainty concerning simulations, it is ascertained that the uncertainty can be captured with Gaussian distribution. Conditional simulation provides for the local variability by creating alternate equiprobable images, and uncertainty is characterised by multiple possibilities that exhibit local variation. By constructing multiple images, one can visualise the differences among models that exhibit ten (10) images of the same distribution. It is observed that the local uncertainty is small and that brought about several images that exhibit similar images, trend, and values at a particular location (narrow distribution), whereas if the local uncertainty is considerable, the differences, in simulated values at a particular location will vary over a wide range. By examining these images, as well

as the local distribution, we can ascertain the uncertainty at each location. If one create a sufficient number of images, one of the images could match the real cause. This is another difference between the conventional estimation process and the simulation process. The conventional estimation process never reproduces reality: it is a filtering process, which removes high-frequency information. On the other hand, in the conditional simulation process, the high-frequency information. as well as the low, is preserved

For Gaussian distribution, once the estimate (mean) and the error variance is known, the entire probability density function is. The assumption of Gaussian distribution makes it very convenient to define the uncertainty by using only two parameters; mean and variance. However, one does not independently verify the validity of simulations and realisations by assumption. If the distribution is non-Gaussian, the error variance may not be enough to represent the uncertainty distribution, which is not the case of the data set in this project.

Some uncertainty can be tolerated even accepted, whereas some uncertainty is undesirable. That is, the uncertainty is weighted differently depending on the problem. The parametric technique defines the uncertainty with Gaussian distribution and also accounts for local variability. Once the surrounding samples are well distributed, the error variance will be proportionately reduced. Once the local error variance is calculated, and assume Gaussian distribution, the local uncertainty is defined. This is consistent with the fact that the maximum local error variance is equal to the variance of the sample. The advantages range from reducing the variability of the sample data set to better describing the local uncertainty. The realisations were ranked based on the knowledge of the estimate mean closeness to the average of the corresponding petrophysical property from logs, the error variance, and the entire probability density function is known. From the realisations, reservoir 1 has average effective porosity ranges from 0.27–0.29, with the best realisation having average effective porosity 0.28 with a variance of 0.0061. Average permeability ranges between 500md – 900md. The best-ranked permeability realisation has an average permeability of 720md with a variance of 0.04231. The average net-to-gross ranges from 0.87–0.995, with the best realisation having an average net-to-gross of 0.98 with a variance of 0.0061.

4.1. Multilayer perceptron neural networks prediction of reservoirs and rock properties

The three-dimensional distribution forecast of rock and reservoir properties in field of study using Multilayer Perceptron Neural Networks (MLPNN) encompass the usage of 3-D seismic attributes was used as input to forecast petrophysical properties such as permeability, and porosity away from well control, and the uncertainty in resulting maps was quantified in terms of their root mean square error (RMSE). Root Mean Square Error is the standard deviation of residual, which is a difference between the predicted values and observed values, i.e., the input and output of the network, respectively. The closer the results is to zero (0) indicate a fit that is more useful for prediction. The resulting reservoir effective porosity mapping was modelled at the root-mean-square-error of 0.0053, with resulting average effective porosity of 0.295. The effective porosity slice on top of reservoirs (Figure 22) revealed the lateral variation of effective porosity across the field with very high effective porosity areas coincide with the delineated regions of interests. Moreover, there are some other relatively high effective porosity zones as observed on these near

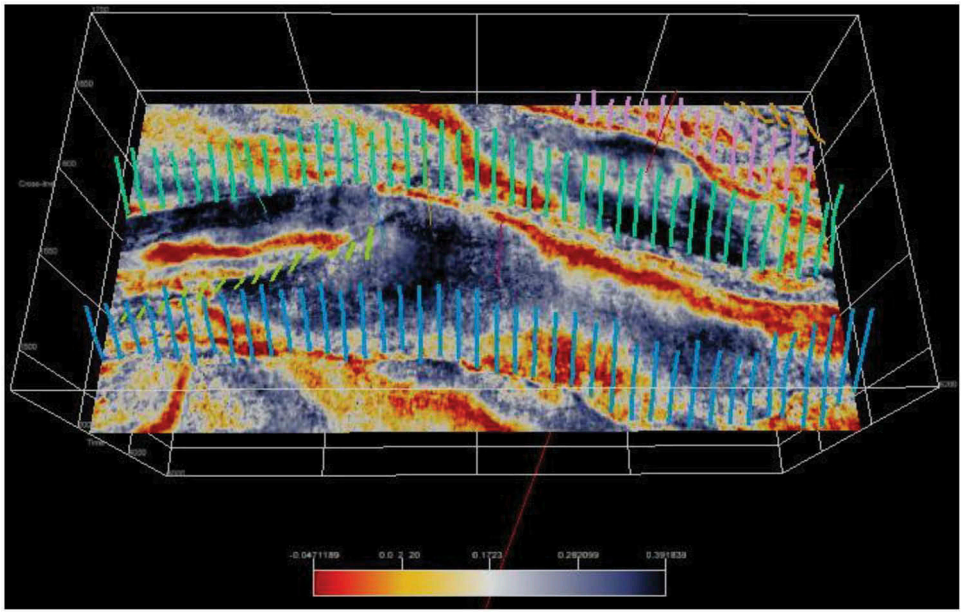

Figure 22. Effective porosity time slice at top of reservoir 2.

reservoirs top slices that were not evident on the seismic attributes. The reservoir lateral permeability variation was modelled at RMS error of 0.03053. The average permeability of the reservoirs as modelled by MLPNN is 735md. The permeability slice on top of reservoirs (Figure 23) revealed the lateral variation of permeability across the field with very high permeability areas coinciding with the delineated regions of interests. The slices revealed some thief zones (channel with high absolute permeability) within and outside the areas with well concentration and region of interest (Figure 23) that were not evident on the seismic attributes. Moreover, hydrocarbon saturation was also modelled at root mean square error of 0.02752 with average of hydrocarbon saturation of 0.69681. The resulting hydrocarbon saturation maps (Figure 24) revealed the lateral variation of hydrocarbon saturation across the field with very high hydrocarbon saturation areas coinciding with the delineated regions of interests. These maps also revealed some other relatively high hydrocarbon saturation zones as observed on the slices of near reservoirs top. The Volume of shale MLPNN mapping was modelled at RMS error of 0.023 with resulting average volume of shale of 0.273. The volume of shale slice on top of reservoirs (Figure 25) revealed the lateral variation of volume of shale across the field with very low volume of shale areas coincide with the delineated regions of interests. Although, the mapped reservoirs are characterised by low volume of shale with some relatively very low volume of shale zones as observed on these near

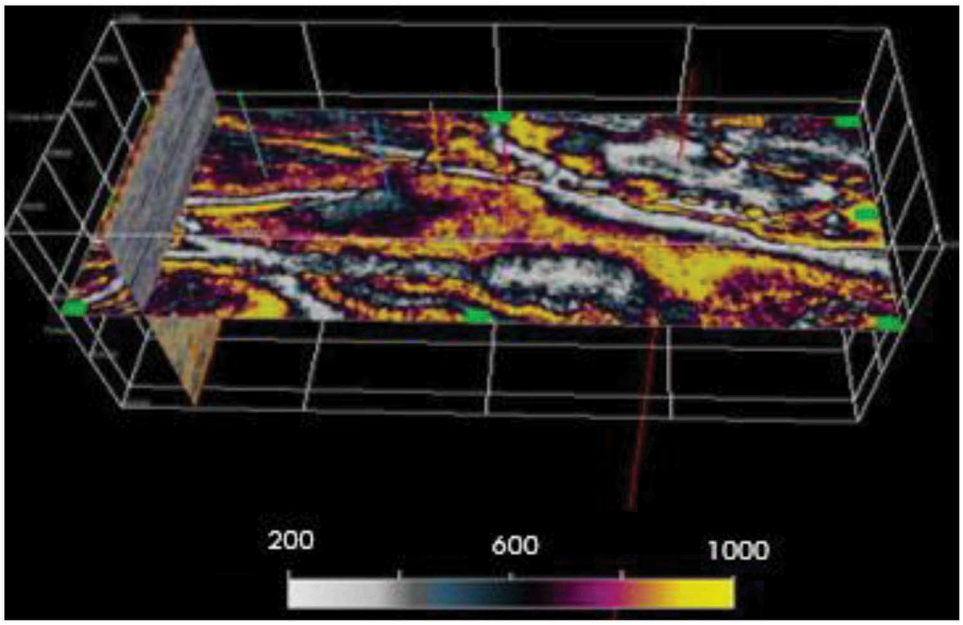

Figure 23. Permeability time slice at top of reservoir 2.

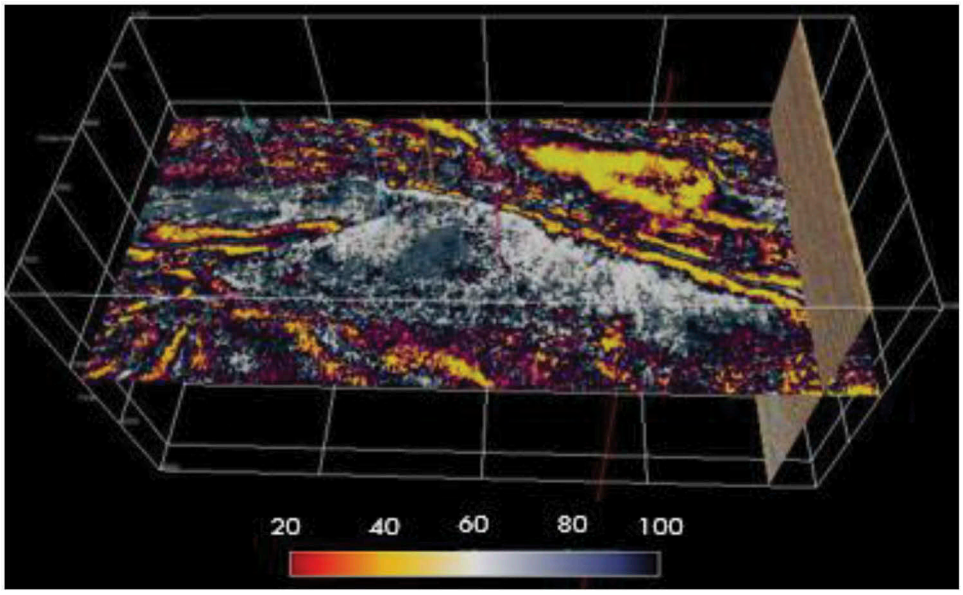

Figure 24. Hydrocarbon saturation time slice at top of reservoir 2.

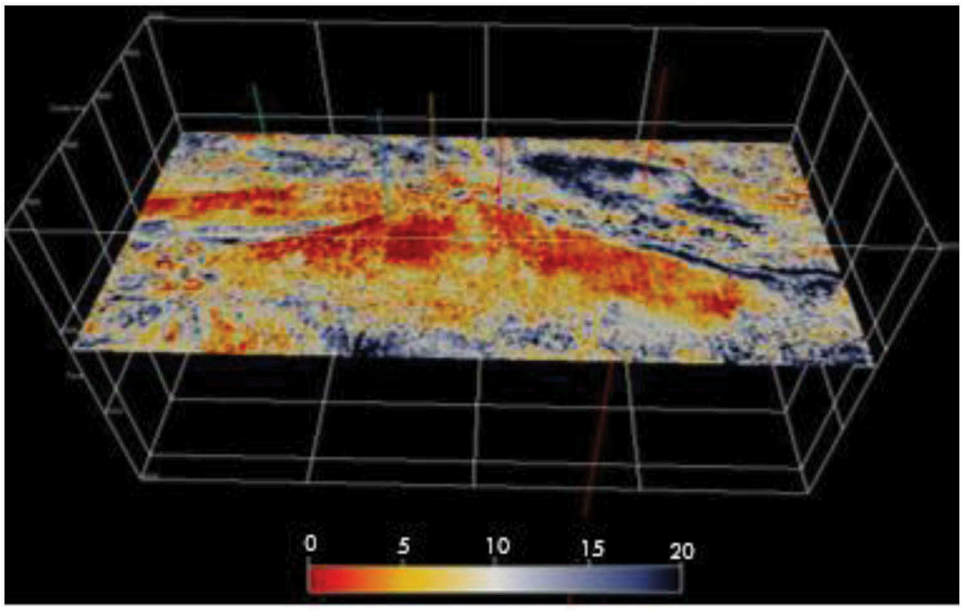

Figure 25. Volume of shale time slice at top of reservoir 2.

reservoirs' top slices. MLPNN modelled map of net-to-gross (NTG) (Figure 26) at RMSE of 0.023 revealed that 82% of the reservoirs has very high of 0.78014. The lateral variation of net to gross across the field with relatively very high NTG values between 0.7 – 1 coincide with the delineated regions of interests. However, the mapped reservoirs are characterised by very low volume of shale zones as observed on the near reservoirs' top slices of volume of shale MLPNN modelled zones.

4.2. Statistical comparative and complementary analysis of MLPNN and geostatistical inversion

Comparative analysis of different techniques and tools used in geomodelling and lateral predictions of the petrophysical properties of interest revealed that both tools explained and honoured well log information satisfactorily (Figure 27(a)). They are both map-based. Figures 4.91a- 4.91d show, Cross-correlation function plot of raw data and multilayer perceptron neural network geomodel data, Cross-correlation and box plot of raw data and multilayer perceptron neural network data, Q-Q plot of Raw data and Q-Q plot of multilayer perceptron neural network modelled data respectively. The multilayer perceptron neural network map-based approach of geomodel petrophysical parameters and lateral prediction provide a very high correlation coefficient of 0.99971 with the base case, Biased Variance 56,918.888, and T-Test 408.029 (Table 1). Figure 27(a–d) show cross-correlation

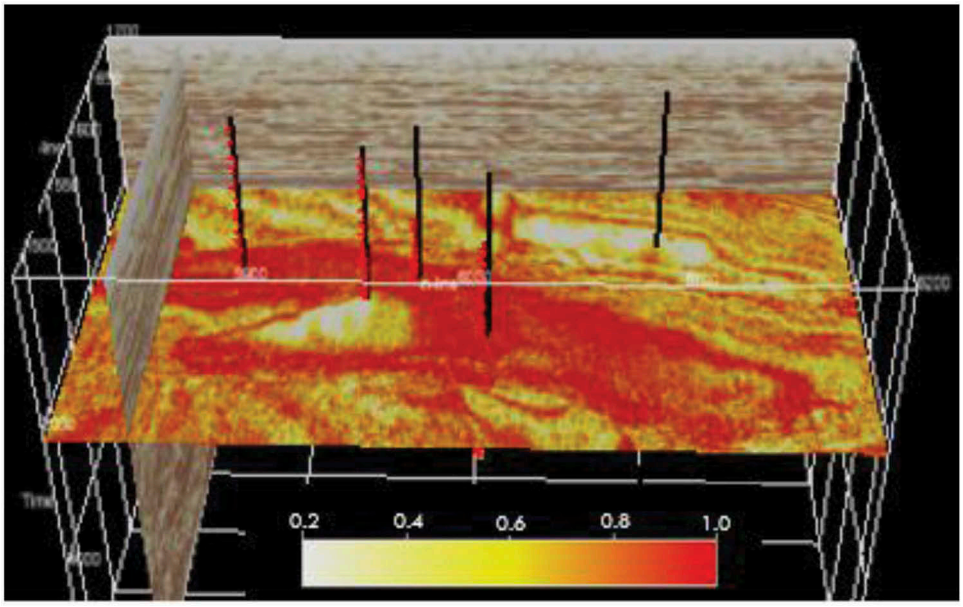

Figure 26. Net to gross time slice at top of reservoir 2.

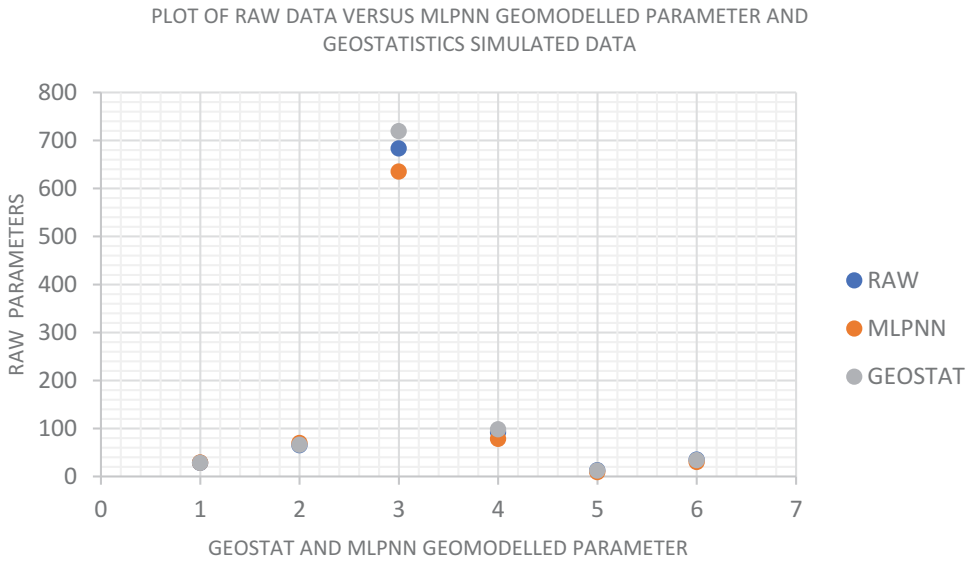

Figure 27. (a)Plot of selected raw data versus MLPNN geomodel parameter and geostatistics simulated data.

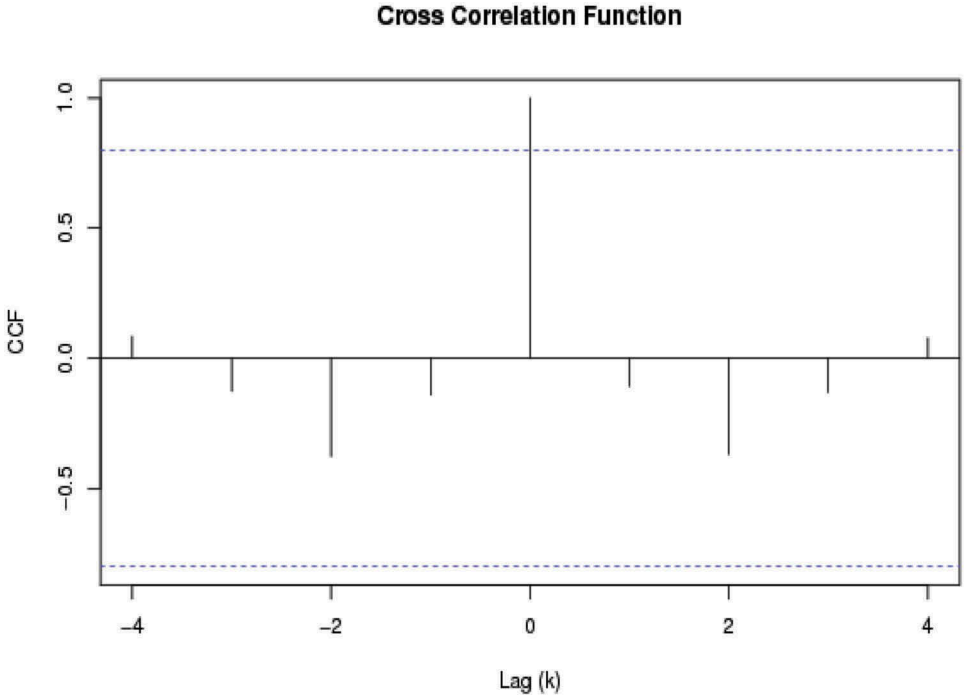

Figure 27. (b) Cross correlation function plot of raw data and geostatistics realised data.

function plot of raw data and geostatistics realised data, cross-correlation and box plot of raw data and geostatistics realised, Q-Q plot of Raw data and Q-Q plot of geostatistics realised data respectively. Geostatistical inversion had a relatively higher correlation coefficient of 0.99998 with the base case, biased variance 56,918.8, and T-Test 408.0297 (Table 2) with the raw estimated petrophysical parameters.

Therefore, geostatistics inversion provides a general improvement in comparison to a multilayer perceptron neural network with raw estimated petrophysical parameters and also dramatically reduces the problems of sparse well coverage. However, the said improvement in the comparison is a function of the initial set conditional parameters for the geostatistical inversion. An inadequate or wrong initial conditional parameters will have an adverse effect in the resulting modelled zones, whereas a multilayer perceptron neural network with no initial condition parameter from the modeller or interpreter because of its "black box" nature will provide a better result in this case.

5. Conclusion

Seismic and borehole log data have been used to demonstrate structural features of identified sand

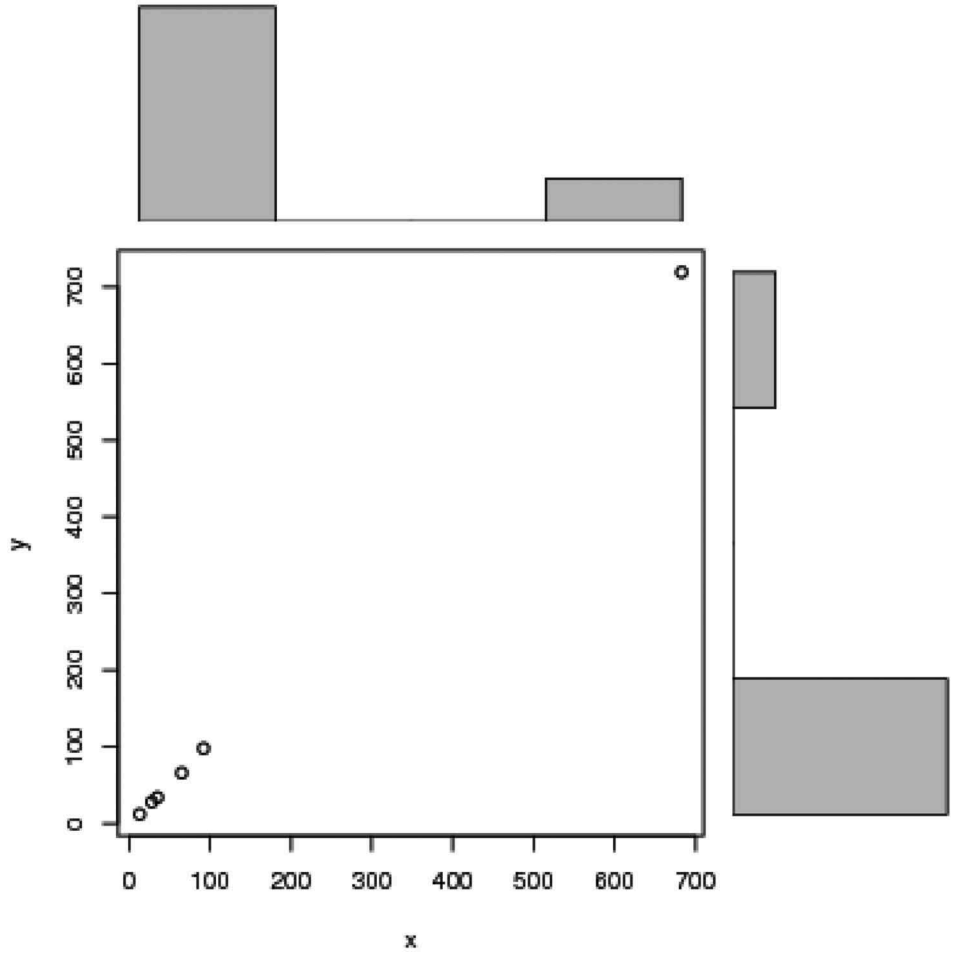

Figure 27. (c). Cross correlation and box plot of Raw data and geostatistics realised.

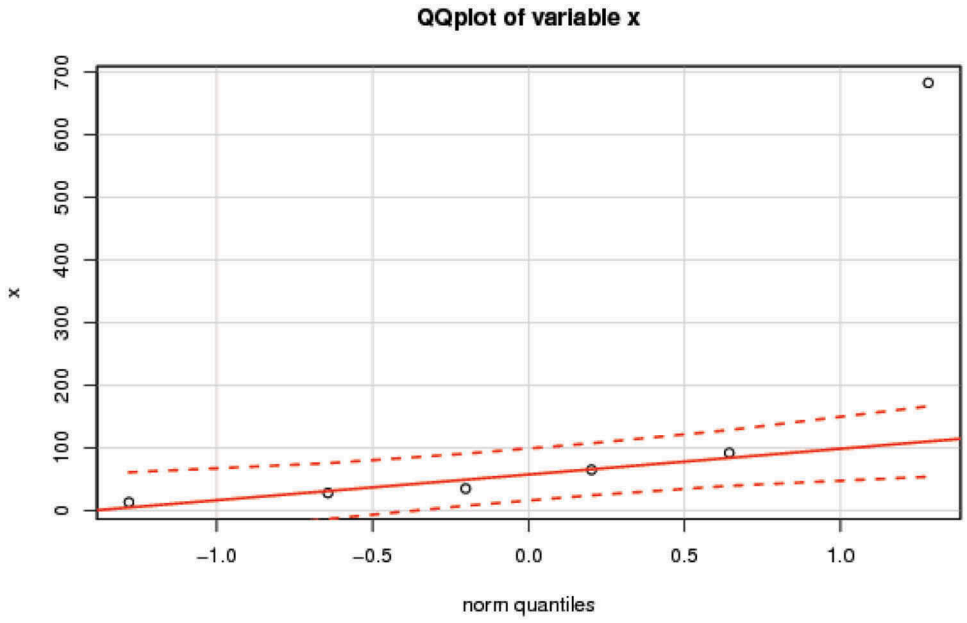

Figure 27. (d). Q-Q plot of raw data.

bodies within the subsurface of the "P" field. This was made possible by creating time and depth structural contour maps of four horizons using the Petrel interpretational tool. The time and depth structure maps show subsurface structural geometry and possible hydrocarbon trapping potential. Four horizons matching to near top of delineated hydrocarbon-bearing sands were mapped and subsequently used

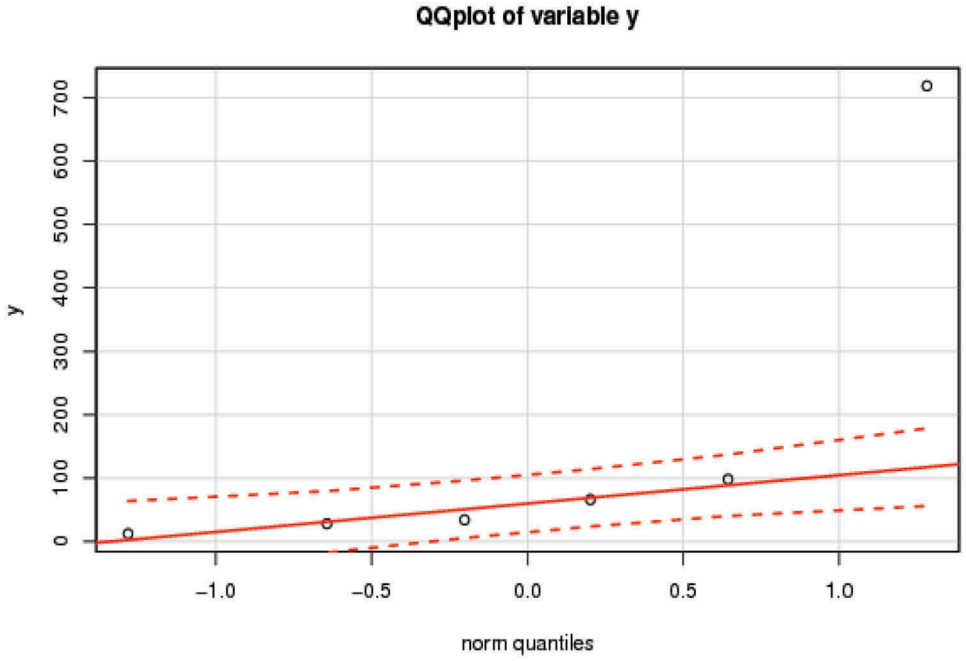

Figure 27. (e).Q-Q plot of geostatistics realised data.

Table 1. Pearson product moment correlation of variable **RAW** versus variable **GEOSTATISTICS.**

Pearson Product Moment Correlation – Ungrouped Data (**Wessa P., (2017)**,)	
Statistic: Variable **RAW** Versus Variable **GEOSTATISTICS**	
Mean	152.666666666667 159.508333333333
Biased	
Biased Variance	56,918.8888888889 63,391.7253472222
Biased Standard Deviation	238.576798722946 251.777134281932
Covariance	72,080.9533333333
Correlation	0.999987987359077
Determination	0.999975974862458
T-Test	408.029757558887
p-value (2 sided)	2.16454446171126e-10
p-value (1 sided)	1.08227223085563e-10
95% CI of Correlation	[0.999884522091943, 0.999,998750437589]
Degrees of Freedom	

Table 2. Pearson product moment correlation of variable **RAW** versus variable **MLPNN.**

Pearson Product Moment Correlation – Ungrouped Data (**Wessa P., (2017)**,)	
Statistic:	Variable **RAW** Versus Variable **MLPNN**
Mean	152.666666666667 141.783333333333
Biased Variance	56,918.8888888889 49,229.0013888889
Biased Standard Deviation	238.576798722946 221.876094676486
Covariance	63,503.3933333333
Correlation	0.999716745413448
Determination	0.999433571060057
T-Test	84.0106307201509
p-value (2 sided)	1.20338377998717e-07
p-value (1 sided)	6.01691889993583e-08
95% CI of Correlation	[0.997280241433355, 0.99997053210023]
Degrees of Freedom	4

to make time maps and then depth structural maps using appropriate check shot data. The shallower reservoirs displayed a blocky gamma-ray log motif, while the deeper sand packages showed a crescentic gamma-ray curve shape. These gamma-ray log motifs probably point to distributary channel and delta marine fringe depositional environments, respectively. Within the paralic Agbada Formation, relatively high readings of deep resistivity curves in the evaluated sand packages indicate the presence of hydrocarbons. Computed petrophysical parameters of the reservoirs in each of the wells show that each formation has varying degree of petrophysical parameters; the average water saturation in these reservoirs is low, ranging from 27% to 41% with a corresponding hydrocarbon saturation ranging from 59% to 73% indicating that the reservoirs contain more hydrocarbon than water in all the seven wells. The reservoirs have the average effective porosity ranging from 27% to 31%, which is an indication of a reservoir with excellent porosity. The MLPNN produced horizon cubes for the areas of interest defined relations that correlate excellently well with three-dimension seismic attributes. MLPNN showed how permeability, porosity, the volume of shale, and hydrocarbon saturation varies away from well control across the entire field. It also revealed some bypassed hydrocarbon sand-rich bedding and some channels that would be of exploration and exploitation interest. Multivariate spatial analysis carried out in the study assisted in having a better understanding of the influence of a secondary variable in stochastic simulation operations. Comparative analysis of different techniques and tools used in geomodelling and lateral predictions of the petrophysical properties of interest revealed that the higher the data density, the better the predictability of MLPNN while geostatistics map-based inversion is not affected by limited numbers of wells provided the initial conditional parameters for the models are correct. However, both tools explained and honoured the

well log information satisfactorily. The MLPNN map-based approach of geomodel petrophysical parameters and lateral prediction provide a very high correlation coefficient of **0.99971** while geostatistics inversion had a relatively higher correlation coefficient of 0.99998 with the raw estimated petrophysical parameters. Therefore, geostatistics inversion provides a general improvement in comparison of the two (2) tools with raw estimated petrophysical parameters and also greatly reduces the problems of sparse well coverage. However, the said improvement in the comparison is a function of the initial set conditional parameters for the geostatistical inversion. Some poor or wrong initial conditional parameters will have a negative effect in the resulting modelled zones, whereas an MLPNN with no initial condition parameter from the modeller or interpreter because of its "black box" nature will provide a better result in this case. The methods also clearly bring out the two distinct channel features which were not evident on structural and RMS attribute map. For better reservoir characterisation and lateral prediction of its petrophysical properties, integration of different map-based prediction tools is encouraged because there is no single prediction tool that can capture in entirety the lateral inhomogeneity of subsurface in the study area. Moreover, the different tool has different inherent merit and demerit, so it is believed that where a particular tool has a weak predictability or delineation deficiency, the other tool will complement and capture the geologic feature(s) of interest. These prediction tools served better as a complementary tool to each other rather than as a comparison tool. Finally, maps generated for lateral variations of petrophysical properties of interest from these different methods are better used together and integrated into decision making as regards analysing of various producing sand units in the study area, which will help formulate a strategy for exploration, exploitation, and development of hydrocarbon resources in the area of study. As inference from the three-dimension seismic interpretation, the studied area offers prospective structurally controlled trapping mechanism/closures for hydrocarbon accumulation, since one well has explored and appraised the south-western sides of the areas of the reservoir especially, more exploitation wells should be drilled to boost hydrocarbon production further and the drilling of the wells should be done to a feasible depth to at, which the OWC will be encountered and for decent, valuable production. Moreover, it is also advisable that the previously known approach given to the interpretation of data set in the exploration of oil and gas be made all-encompassing and in-depth to account for subtle inconsistencies and discrepancies unique to different data. Over modelling or training of data sets is a subtle error and is often a challenge in the geostatistical analysis because it is a prediction/interpolation and extrapolation tool. Therefore, it is recommended that this should be handled carefully, and the use of correct modelling parameters must be professionally advised. An integrated approach to data analysis is the best, and it is therefore recommended. It is recommended that scale variations be carefully handled in executing a work like this.

5.1. Recommendations

A combination of suites of well-logs and 3-dimensional seismic data in the multivariate analysis utilising geostatistics and the neural network has added another dimension in the science of interpretation of mature oil fields. This has helped in imaging lateral and vertical inhomogeneities of the reservoirs harbouring oil and gas in the field. In this project, two zones designated as a region of interests 1 and 2 have been found prospective for the drilling of development wells to increase reserve in this field. Furthermore, the significant faults should also be subjected to a fault seal analysis to ascertain their trapping integrity and mechanism to minimise the risk of drilling dry wells. Biostratigraphic studies are also useful to map accurate lithology, depositional sequences, and environment of sediment deposition. These parameters have a significant influence on oil and gas accumulation and production.

Disclosure statement

No potential conflict of interest was reported by the author.

References

Avbovbo AA. 1978. Tertiary lithostratigraphy of niger delta. American Association of Petroleum Geologists Bulletin. 62:295–300.

BP. 2014. Statistical review of world energy. http://www.bp.com/

Caers J, Strebelles S, Payrazyan K. 2003. Stochastic integration of seismic data and geologic scenarios- A west Africa submarine channel saga. Leading Edge. 23(3):281–289.

Chambers RL, Yarus JM. 2002 June. Quantitative use of seismic attributes for reservoir characterization. CSEG Recorder. 32(2):14–25.

Chambers RL, Zinger MA, Kelly MC. 1994. Constraining geostatistical reservoir description with 3D seismic data to reduce. American Association of Petroleum Geologists Computer Application in Geology. 3:234–253.

Damuth JE. 1994. Neocene gravity tectonics and depositional processes on the deep Niger Delta continental margin. Marine and Petroleum Geology. 11(3):320–345.

Daniel PH, James SS, John AQ. 2001. Use of multiattribute transforms to predict log properties from seismic data. SEG. 201:220–236.

David M, Chaosheng Z, Owen TC. 2004. Geostatistical analysis and hazard assessment of soil in silver-mines areas, Ireland. Environmental Pollution. 127:239–248.

Evamy B, Haremboure J, Kamerling P, Knaap W, Molloy F, Rowlands P. 1978. Hydrocarbon habitat of tertiary niger

delta. American Association of Petroleum Geologists Bulletin 62:1–39.
Fogg AN. 2000. Petro-seismic classification using neural networks: UK onshore; 70th Forecasting and monitoring. The Leading Edge. 16:445–456.
Frykman P, Deutsch CV. 2002. Practical application of geostatistical scaling laws for data integration. Petrophysics. 43 (3):153–171.
Hampson DP, Schuelke JS, Quirein JA. 2001. Use of multiattribute transforms to predict log properties from seismic data. SEG. 54:220–236.
Helle HB, Bhatt A, Ursin O. 2001. Porosity and permeability prediction from wireline logs using artificial neural networks: a North Sea case study. Geophysical Prospecting. 49:431–444.
Hoffman B, Caers J. 2005. Regional probability perturbations for history matching. Journal of Petroleum Science and Engineering. 46(1):53–71.
Journel AG. 1994. Stochastic modeling and geostatistics: principles, methods and case studies. American Association of Petroleum Geologists Computer Applications in Geology. 3:19–20.
Liu Y, Harding A, Abriel W, Strebelle S. 2004. Multi-point simulation integrating wells, 3-D seismic and geology. America Association of Petroleum Geologist Bulletin. 58 (7):905–921.
Pramanik AG. 2004. Estimation of effective porosity using geostatistics and multiattribute transforms A case study. SEG 44:352–372.
Rafael EB, Reinaldo JM. 2002. From 3D seismic attributes to pseudo-well-log volumes using neural networks: practical considerations. SEG 37:996–1001.
Robinson G. 2001 January 01. Stochastic seismic inversion applied to reservoir characterization. CSEG Recorder 23:36–40.
Russell B. 1997. Multiattribute seismic analysis. SEG 34:1439–1444.
Schultz PS. 1994. Seismic-guided estimation of log properties (Part 1: a data-driven interpretation methodology. SEG 24:305–310.
Shannon PM, Naylor N. 1989. Petroleum basin studies. London: Graham and Trotman Limited; p. 153–169.
Short K, Stauble A. 1967. Outline of geology of niger delta. American Association of Petroleum Geologists Bulletin. 51: 761–779.
Skolen JO, Merz R, Bloschl G. 2006. Top-kriging geostatistics on stream networks. Journal of Hydrology and Earth System Sciences. 10:277–287.
Stacher P. 1995. Present understanding of the Niger Delta hydrocarbon habitat. In: Oti MN, Postma G, editors. Rotterdam: Geology of Deltas Balkema 32: 257–267.
Strebelle S 2001. Sequential Simulation- Drawing structures from training images. Unpublished PhD. Thesis, Department of Geological and Environmental Sciences, Stanford University, USA,200 p.
Strivastava RM. 1994. An overview of stochastic methods for reservoir characterization. American Association of Petroleum Geologists Computer Application in Geology. 3:88.94.
Tonn R. 2002. Neural network seismic reservoir characterization in a heavy oil reservoir. The leading edge 21 (3):309–312.
Walls JD. 2002. Seismic reservoir characterization of U.S. Midcontinent fluvial system using rock physics, post-stack seismic attributes, and neural networks. p.428–436.
Weber KJ. 1986. Hydrocarbon distribution patterns in nigerian growth fault structures controlled by structural style and stratigraphy. American Association of Petroleum Geologists Bulletin. 70:661–662.
Weber KJ, Dakoru EM. 1975. Petroleum geology of the niger delta: Proceedings of the Ninth World Petroleum Congress, Geology, London, Applied Science Publishers, Ltd., 2nd Edition, pp. 210–221.
Webster R, Oliver MA. 2007. Geostatistics for environmental scientists, 2nd Edition. Willey- Lackwell 33: 333.
Wessa P. 2017. Cross Correlation Function Software, Office for Research Development and Education. https://www.wessa.net/rwasp_cross.wasp/